



OPEN ACCESS

EDITED BY

Jose Luis Cortina,
Universitat Politecnica de Catalunya, Spain

REVIEWED BY

Marek Bryjak,
Wroctaw University of Technology, Poland
Marcos Fallanza,
University of Cantabria, Spain

*CORRESPONDENCE

Aydın Cihanoğlu,
✉ aydin.cihanoğlu@ege.edu.tr
Enver Güler,
✉ enver.guler@atilim.edu.tr
Nalan Kabay,
✉ nalan.kabay@ege.edu.tr

RECEIVED 09 April 2024

ACCEPTED 06 August 2024

PUBLISHED 21 August 2024

CITATION

Gül TF, Akalın M, Dönmezler EN, Bolat A,
Cihanoğlu A, Güler E and Kabay N (2024)
Review on reverse electrodialysis process—a
pioneering technology for energy generation by
salinity gradient.
Front. Membr. Sci. Technol. 3:1414721.
doi: 10.3389/frmst.2024.1414721

COPYRIGHT

© 2024 Gül, Akalın, Dönmezler, Bolat,
Cihanoğlu, Güler and Kabay. This is an open-
access article distributed under the terms of the
[Creative Commons Attribution License \(CC BY\)](https://creativecommons.org/licenses/by/4.0/).
The use, distribution or reproduction in other
forums is permitted, provided the original
author(s) and the copyright owner(s) are
credited and that the original publication in this
journal is cited, in accordance with accepted
academic practice. No use, distribution or
reproduction is permitted which does not
comply with these terms.

Review on reverse electrodialysis process—a pioneering technology for energy generation by salinity gradient

Taha Furkan Gül¹, Minel Akalın¹, Eda Nur Dönmezler¹,
Ahmet Bolat¹, Aydın Cihanoğlu^{1,2*}, Enver Güler^{3*} and
Nalan Kabay^{1*}

¹Chemical Engineering Department, Ege University, İzmir, Türkiye, ²Aliağa Vocational School, Refinery and Petrochemical Department, Ege University, İzmir, Türkiye, ³Chemical Engineering Department, Atılım University, Ankara, Türkiye

Blue energy obtained by salinity gradient can be generated by mixing two saline solutions having different salt concentrations. According to researchers working in this area, about 80% of the current global electricity demand could potentially be covered by this energy source. There are basically two membrane technologies so-called pressure-retarded osmosis (PRO) and reverse electrodialysis (RED) that are capable to generate electrical energy from salinity gradient. The pressure driven PRO process is more suitable for energy generation from highly concentrated brines. However, RED is more favorable for power generation by mixing seawater and river water. In RED process, ion exchange membranes (IEMs) placed between two electrodes in a stack were employed for transport of ions. Thus, an electrical current is obtained at the electrodes by electron transport through redox reactions. This review gives an overview of RED as a pioneering technology for salinity gradient energy (SGE) generation. The review summarizes the recent improvements of IEMs employed for RED studies, membrane fouling and RED stack design.

KEYWORDS

salinity gradient energy, blue energy, reverse electrodialysis, ion exchange membranes, fouling

1 Introduction

The creation of sustainable and renewable energy conversion technologies is becoming increasingly crucial as environmental issues such as pollution and global warming gain momentum. The current renewable energy technologies include geothermal water, wind power, photovoltaics and hydropower (Archer and Jacobson, 2005; Zarfl et al., 2015; Moya et al., 2018; Dambhare et al., 2021). The energy harvesting from these technologies strongly depends on the climate and time. This drawback limits the use of these technologies. However, salinity gradient energy (SGE) is validated as a sustainable and non-polluting energy source. Further, this technology is climate and time-independent technology.

There are two significant technologies in capturing SGE. These are pressure-retarded osmosis (PRO) and reverse electrodialysis (RED). Energy harvesting is based on the use of membranes in these technologies. In PRO, semi-permeable membranes are used, and the transport mechanism is based on the water molecules' transport. On the other hand, in

RED, ion exchange membranes (IEMs) are used, and the transport mechanism is based on the charged species' transport (Post et al., 2007).

In recent years, scientists and private sector specialists have attracted great interest in the RED technology since this technology converts the seawater and river water mixing to energy. In this technology, anions and cations in the seawater are transported to the river water side by anion exchange membranes (AEMs) and cation exchange membranes (CEMs), respectively. The ions transport creates a potential known as Nernst potential, and potential is converted into energy by redox reactions in the electrodes. Monovalent ion selectivity and permselectivity of IEMs are among the most significant features that affect the efficiency of the RED technology. Further, low membrane resistance and high ion exchange capacity (IEC) are responsible for energy efficiency (Post et al., 2007). Until 2012, researchers have used commercial IEMs in the RED system, and these membranes have not met the demands of RED requirements. For the first time in the literature, Guler et al. (Guler et al., 2012) synthesized tailor-made AEMs considering the RED requirements for energy harvesting from the RED system. After that research, a great effort on the IEMs synthesis for the RED system has been made in the literature. Beyond the membrane properties, the RED system operating parameters such as temperature, salinity, flow velocity, flow modes, presence of multivalent ions and organic foulants, the number of membrane pairs, and spacer thickness and geometry are the main system design variables influencing the RED performance.

The other critical issue in the RED technology is sustainability in terms of economic and financial feasibility. Almost a decade ago, the ion exchange membranes price was 50 €/m², and energy harvesting from the RED system was more expensive than other energy sources, such as solar and wind power. Nowadays, however, the use of cheap raw materials and economically feasible manufacturing procedures has reduced membrane prices to around 4.3 €/m². The electricity costs were predicted to be 0.17 €/kWh in the RED system with a membrane of 4.3 €/m², operating on seawater/river water. This scenario shows that RED could compete with solar and wind power generation systems at costs as low as 0.14 €/kWh (Tufa et al., 2018).

In this review study, the structure and synthesis approaches of IEMs are explained in detail, and the requirements of membranes for the RED system are comprehensively discussed. The effect of multivalent ions' presence in the feed water on the membrane transport mechanisms and their performance is discussed. The fouling tendency and mechanisms of membranes are explained by considering the presence of organic, inorganic, and biological foulants. The approaches that provide the antifouling behavior to the membranes are presented in detail. Lastly, the RED stack design considering spacer thickness, geometry, and flow modes is comprehensively discussed, and the effect of these parameters on the membrane performance is explained in detail.

2 Recent developments of anion exchange membranes for RED applications

AEMs are considered as membranes with selective permeability for anions since they include positively charged groups that only let

TABLE 1 Functional groups of AEMs (Xu, 2005; Zuo et al., 2022).

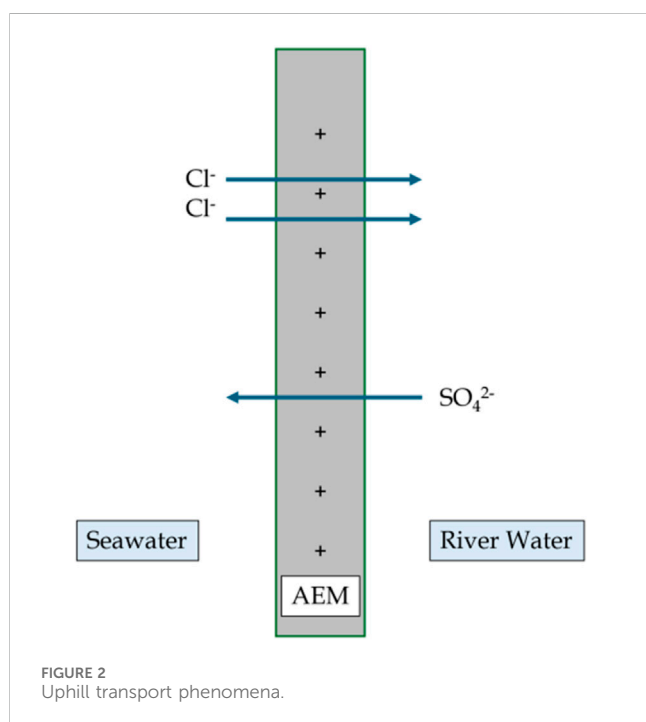
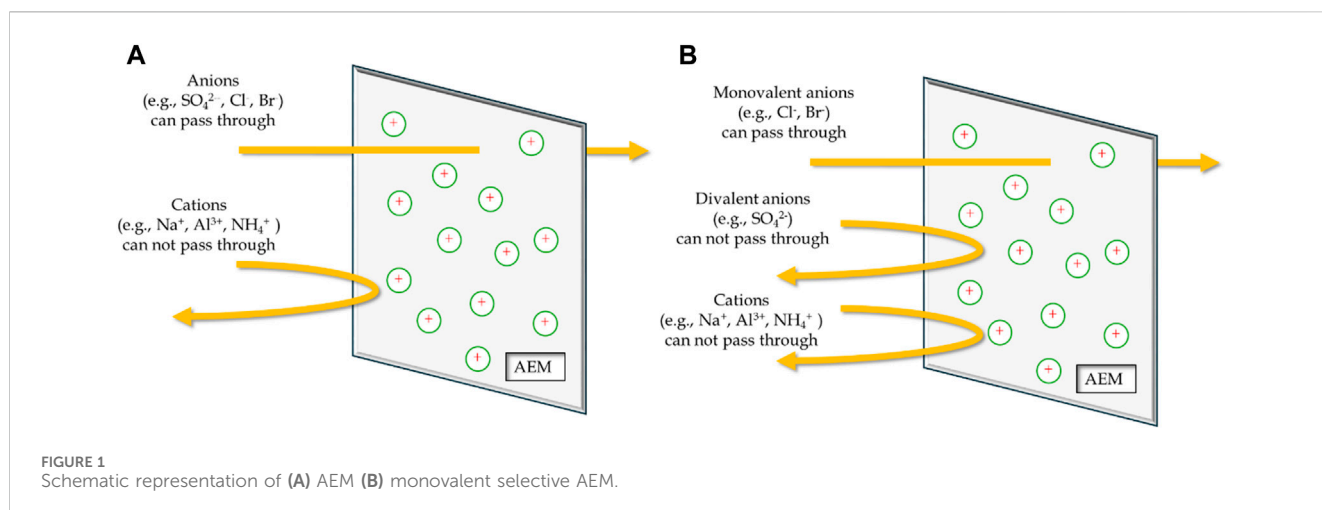
$-\text{NH}_3^+$	Ammonium
$-\text{NRH}_2^+$	Secondary amine
$-\text{NR}_2\text{H}^+$	Tertiary amine
$-\text{NR}_3^+$	Quaternary amine
$-\text{PR}_4^+$	Phosphonium group
$-\text{SR}_3^+$	Sulfonium group

anions to pass through (Table 1). A main chain joined within a polymer structure and a side chain made up of a positively charged group linked through chemical bonds form a channel that provides a path for anions to travel through (Xu, 2005). As shown in Figure 1, this structure allows anions to pass through selectively while preventing cations from moving.

Effective AEMs necessitate high electrical conductivity, superior thermal stability, mechanical strength and high permselectivity. However, achieving this perfection practically is challenging due to factors such as membrane water content influencing permselectivity significantly (Varcoe et al., 2014; Yang et al., 2020). Generally, increased water content leads to membrane swelling and subsequent reduction in dimensional stability, strongly impacting membrane permselectivity. Diminished dimensional stability results in reduced permselectivity. Decreasing surface hydrophilicity may reduce water content and thus improve membrane dimensional stability, but it may also increase membrane resistance. Elevated resistance of membranes leads to lower conductivity, which reduces energy efficiency and increases costs (Fan et al., 2020).

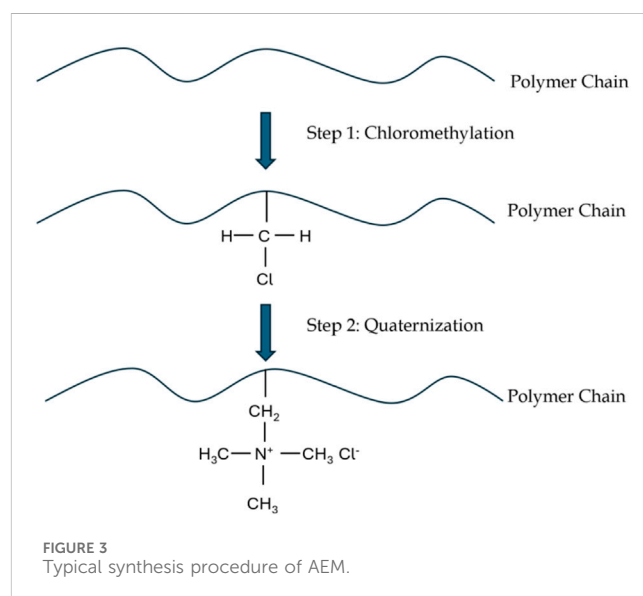
The ionic resistance and permselectivity properties of quaternary ammonium-functionalized AEMs using poly (sulfone) and poly (phenylene oxide) (PPO) polymer frameworks were evaluated by Geise et al. (Geise et al., 2013). They characterized these properties in aqueous NaCl solutions, identifying their sensitivity to the polymer's water content. They were able to change the polymers' ionic resistance by orders of magnitude by varying the water content and nanophase separation of the polymers, and they observed variations across different polymer backbone types. Permselectivity demonstrated a response to both water content and fixed charge concentration, typically declining as the polymers' water volume fraction increased. Through their analysis, they developed structure-property relationships, establishing connections between the transport properties and the fixed charge concentration of the membranes along with their water content.

Furthermore, the lack of appropriate selective IEMs poses a challenge for the application of RED technology using real water sources, particularly when dealing with various ions especially multivalent ions in seawater. These ions cause RED performance to decrease in terms of power density (P_d) and open-circuit voltage (OCV) (Moya, 2020). This decline is primarily linked to the increased resistance in the IEMs and diminished permselectivity. Additionally, as depicted in Figure 2, an uphill transport phenomenon is mainly attributed to the transport of multivalent ions contrary to the concentration gradient (Post et al., 2009; Tufa et al., 2018).



Thus, selectivity towards specific ions is one of the key electrochemical characteristics influencing RED performance of membranes. The selectivity during the RED process is mainly provided by tailor-made IEMs. Monovalent ion selective membranes, for example, as shown in Figure 1B, can separate monovalent ions from solutions like seawater and river water that contain both monovalent and multivalent ions (Guler et al., 2014).

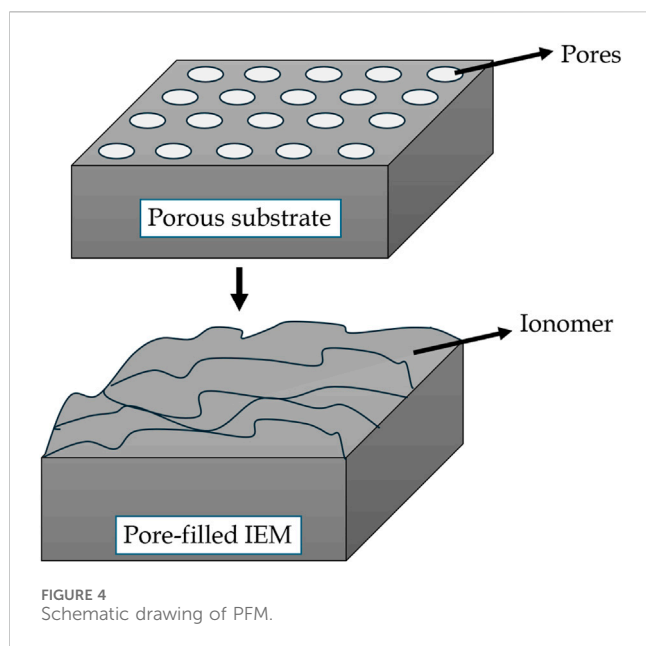
As shown in Figure 3, the standard procedure for synthesizing AEMs consists of two steps: first, chloromethylation, and then, quaternization, which introduces quaternary ammonium groups. However, these methods frequently rely on using multiple hazardous chemicals. For instance, it is well known that an often used substance in chloromethylation, chloromethyl methyl ether, causes cancer in humans. A viable resolution to this issue involves



bypassing chloromethylation and directly engaging in the quaternization of nitrogen-containing polymers (Qaisrani et al., 2018).

Guler et al. (2012) developed and tested poly (epichlorohydrin) (PECH) based AEMs, specifically designed for RED applications for the first time, employing an environmentally friendly solution which is a casting approach using 1,4-diazabicyclo [2.2.2] octane (DABCO) for amination and simultaneous crosslinking. Specifically focusing on developing AEMs, a safer and more environmentally friendly approach was proposed, utilizing halogenated polymers like PECH as the initial material. A tertiary diamine (DABCO) was used through amination to introduce ion exchange groups and crosslink the polymer membrane simultaneously. These AEMs combined with commercial CEMs (CMX) in the RED system resulted in a P_d of 1.27 W/m².

Afterwards, numerous studies involving various methods have been conducted to obtain high performance AEMs with characteristics such as monovalent selectivity, antifouling behavior, high permselectivity, and low resistance. Those studies



aimed for enhancing the performance of AEMs for RED applications. Several of them suggest different synthesis and modification techniques for enhancing AEMs' effectiveness. These methods include layer-by-layer deposition, pore filling, dip coating, and UV-induced, oxidative self-polymerization procedures (Faraj et al., 2012; Kim et al., 2016; Zhao et al., 2018; Zhao et al., 2019; Sankar et al., 2022). This section of this review focuses on improving the performance of AEMs, a critical component of the RED system, by exploring synthesis conditions, surface modification techniques, studies conducted by various commercial AEMs, and recent advancements in tailor-made AEMs for RED applications.

2.1 Pore-filling membranes

Pore-filled membranes (PFMs) consist of a porous substrate that is chemically inert and mechanically robust, along with a polymer containing ion-exchange groups (like polyelectrolytes or ionomers) filling the pores. Figure 4 demonstrates the fabrication principle of the PFMs. These membranes exhibit the benefit of offering high ion conductivity and outstanding mechanical property. Furthermore, the mechanically robust porous substrate effectively prevents undesirable excessive swelling of the resulting membrane (Kang, 2013).

Choi et al. (2018) investigated the creation of new quaternary ammonium groups within an AEM via the Michael-type addition reaction between catechol and DABCO molecules under alkaline conditions. AEMs were synthesized by utilizing the pore-filling technique to incorporate electrolytes (vinyl benzyl trimethylammonium chloride, or VBTMA), catechol-containing dopamine methacrylamide (DMA), and ethylene glycol diacrylate as a crosslinker into a porous substrate.

After examining the effects of DMA and anion exchange monomer concentrations on the characteristics of the resultant membranes, it was confirmed that the pore-filling AEM with the most favorable properties could be used in a RED system (Figure 5).

Remarkably, the DABCO-bound AEM showed a notable improvement in permselectivity (94%) and a great decrease in area resistance ($0.4 \Omega \text{ cm}^2$). Adjusting the concentrations of VBTMA and DMA and establishing new bonds between DMA and DABCO allowed for manipulation of the electrochemical characteristics of the AEMs. This membrane possessing the most favorable properties demonstrated theoretical (4.31 W/m^2) and practical (1.52 W/m^2) power densities during RED processes, surpassing those of a commercial membrane, Neosepta AMX (3.25 and 1.29 W/m^2), by 33% and 18%, respectively.

Later, Lee et al. (2019) developed highly efficient and cost effective AEMs for RED using low-cost polystyrene (PS) and PPO as base materials. In that study, a diamine, serving as a crosslinking agent, was successfully employed to strengthen the bonds between ionomers to enhance mechanical durability. Additionally, the mechanical properties were optimized by embedding ionomers into the polyethylene (PE) matrix support. The atmospheric plasma treated PE matrix membrane facilitated effective ionomer impregnation, improving ionomer-matrix membrane compatibility. As a result of this study, crosslinked quaternary aminated PS (QPS) and quaternary-aminated PPO (QPPO) based PE-supported AEMs were obtained. These AEMs (PErC(5)QPS-QPPO) have greater electrochemical characteristics for RED. The resistance value is substantially lower than the commercial AEM, AMV (Selemion™). Although their thin structures, PErC(5)QPS-QPPO has a transport number equivalent to AMV and has shown accelerated chemical durability in tests. When compared to the AMV membrane, the RED stack performs exceptionally well, with a maximum P_d of 1.82 W/m^2 , which is 20.7% greater. The findings indicate that the PErC(5)QPS-QPPO membrane is a viable alternative AEM option for RED systems, outperforming AMV.

Later, using a pore filling technique, Song et al. (Song et al., 2022) developed thin reinforced AEMs with exceptional chemical and physical stability. These novel membranes were made by impregnating a porous PE substrate with functional monomers, then *in situ* polymerization and further treatments were carried out. These AEMs were unique because of their dual crosslinking reaction, which allowed them to maintain a high IEC and limited swelling at the same time. These AEMs performed better than commercial IEMs in terms of mechanical features, exhibiting tensile strength surpassing 120 MPa and low electrical resistance of less than $1 \Omega \text{ cm}^2$. When tested in the RED system, their performance was apparently better than that of the commercially available AMX membrane.

2.2 Mixed matrix membranes

Mixed matrix membranes (MMMs) are considered highly promising heterogeneous membranes because they offer a wide range of possibilities in blending various inorganic nanoparticles and organic polymers to attain specific membrane properties (Figure 6) (Kickelbick, 2003). The inorganic phase was chosen to enhance ion conductivity while also improving the membrane's thermal, chemical, and mechanical properties. On the other hand, the organic phase was chosen specifically to improve flexibility of the membrane (Hagesteijn et al., 2018).

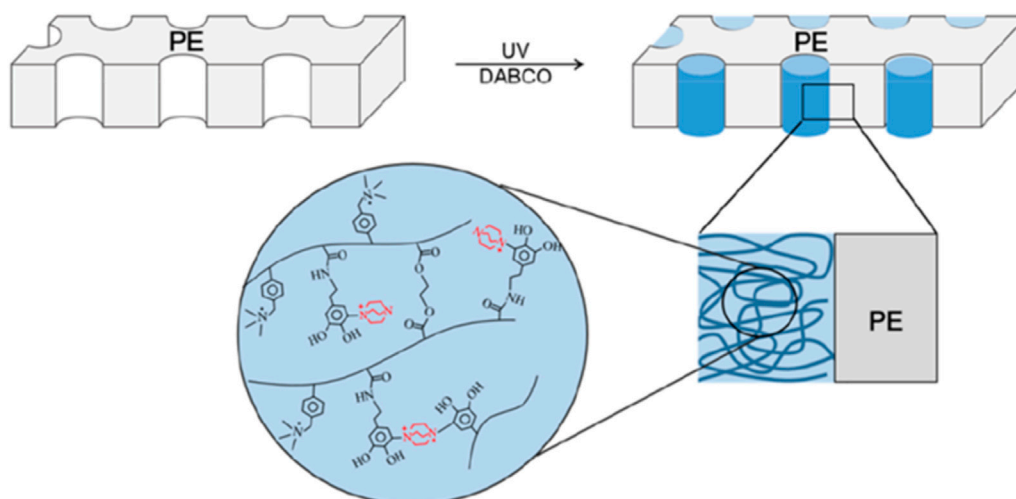


FIGURE 5 A scheme depicting the structure of the PFM formed through the interaction between DMA and DABCO. Reproduced from Reference (Choi et al., 2018) with permission. (Copyright © 2018, American Chemical Society).

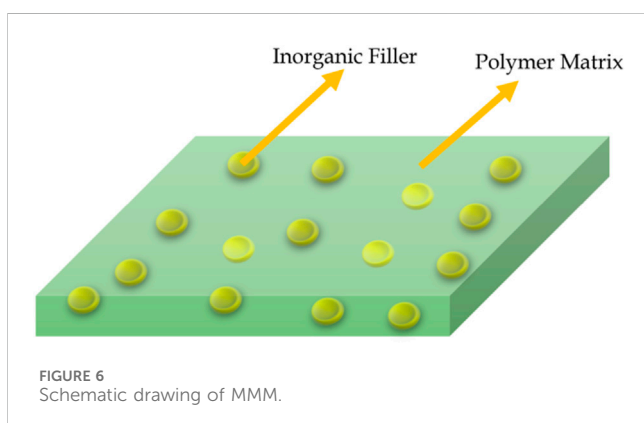


FIGURE 6 Schematic drawing of MMM.

Nemati et al. (2015) synthesized polyvinyl chloride based mixed matrix heterogeneous AEMs and investigated the influence of TiO_2 nanoparticle concentration on membrane properties, focusing on IEC, membrane potential, transport number, permselectivity, ionic permeability, flux, and membrane area resistance. Initially, increasing TiO_2 nanoparticle concentration led to a rise in IEC, followed by a slight decrease, resulting in enhanced membrane potential, transport number, and permselectivity. This trend suggests that higher nanoparticle concentration may restrict access to ion exchange functional groups while optimizing ion transfer channels within the membrane. Moreover, elevated TiO_2 nanoparticle concentration improved membrane's ionic permeability and flux but further increase reduced both parameters. Additionally, the increase in TiO_2 nanoparticle concentration decreased membrane area resistance, indicating enhanced membrane conductivity. These findings highlight the complex interplay between nanoparticle concentration and membrane properties, providing insights into optimizing membrane performance in various applications. Although these findings were obtained in an electro dialysis oriented study, the

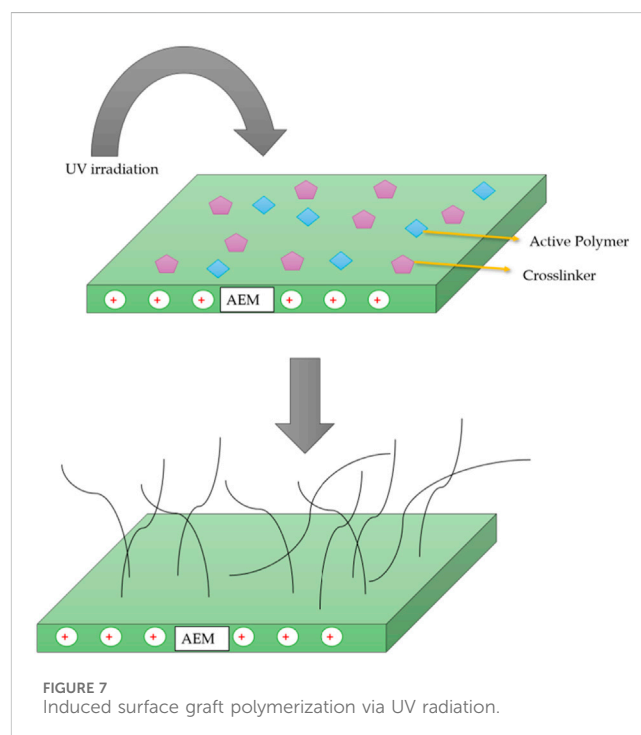


FIGURE 7 Induced surface graft polymerization via UV radiation.

results demonstrate promising potential for TiO_2 nanoparticle infused mixed matrix AEMs in the RED system due to their hydrophilic nature with antifouling properties, increased permselectivity, and reduced area resistance values.

2.3 Surface polymerization

Induced surface graft polymerization via UV radiation (Figure 7) is an effective technique for enhancing the properties of hydrophobic membranes. This method provides membranes with

hydrophilic characteristics without causing damage to the primary membrane material and concurrently conferring antifouling properties at a low cost (Deng et al., 2009).

Radiation-grafted AEMs (RG-AEMs) exhibit high conductivity, but non-crosslinked RG-AEMs typically display undesirable swelling and low permselectivity for RED systems. Crosslinking can improve permselectivity and reduce swelling, yet it can also decrease ion conductivity. Therefore, to attain a suitable balance of membrane properties, the degree of crosslinking must be managed. Crosslinking in RG-AEMs can occur in two ways: either in the amination stage by adding a diamine next to a monoamine, or in the grafting stage by adding divinyl monomers alongside monomers (Bance-Soualhi et al., 2021).

Bance-Soualhi et al. (2021) investigated the impact of this crosslinking step on RG-AEMs. They performed crosslinking on the AEM using two different methods. In one method, they utilized a diamine crosslinker (N,N,N',N'-tetramethyl-1,6-hexanediamine (TMHDA)) during the amination step, while in the other method, they used divinylbenzene (DVB) as a crosslinking agent during the grafting stage. When a TMHDA was used instead of DVB as a crosslinking agent during the amination step, membrane resistance was less negatively impacted and permselectivity was more positively impacted. Considering the higher degree of reduction in swelling achieved with DVB crosslinking, it might be deemed more suitable for other applications. However, they recommended utilizing TMHDA during the amination step when developing crosslinked RG-AEMs for use in RED.

Golubenko et al. (2019) developed a novel AEM by chloromethylating PS and then quaternizing it within graft copolymer films based on UV-oxidized polymethylpentene. Their focus was on studying the chloromethylation kinetics and the impact of reaction conditions on membrane properties. By altering the PS content and crosslinking degree resulted in AEMs with IECs ranging from 1.1 to 2.9 mmol/g and anion transport numbers between 91.0% and 95.5%.

Golubenko et al. (2021) tested radiation created functionalized PS-based graft IEMs for the first time in a RED system. The performance of these AEMs, which were grafted onto UV-oxidized polymethylpentene films and based on quaternized/chloromethylated poly (styrene-co-divinylbenzene) used alongside sulfonated CEMs, was compared with that of other commercial IEMs, namely, FujiFilm® Type 1 and Type 2, and RALEX®. In a laboratory-scale RED system, the high-selectivity graft membranes, created using a copolymer with a surface coating degree of 10% and a grafting degree of 47%, exhibited the highest P_d (2.1 W/m²).

3 Recent developments of cation exchange membranes for RED applications

CEMs, consist of a dense polymer layer comprising crosslinked polymer chains with negatively charged groups, and they are commonly employed to separate electrolytes in electrochemical systems (Luo et al., 2018). Table 2 depicts the typical negatively charged fixed functional groups of CEMs.

Since negatively charged groups are fixed to CEM, anions are rejected by the negative charge and cannot permeate through the

TABLE 2 Functional groups of CEMs (Luo et al., 2018).

-SO ₃ H	Sulfonic acid
-COOH	Carboxylic acid
-PO ₃ H ₂	Phosphorous acid
-CF ₂ SO ₃ H	Perfluorosulfonic acid
-CF ₂ COOH	Difluoroacetic acid
-Phenolic OH	Phenols
-C(CF ₃) ₃ OH	Trifluoroacetic acid

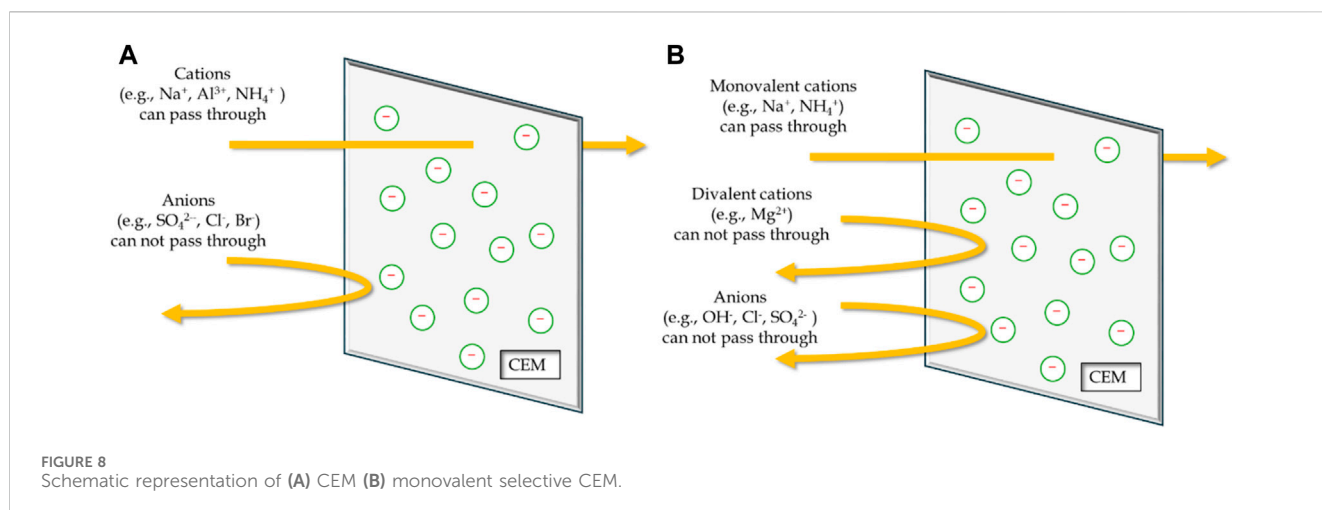
CEM. This is because CEMs are only permeable by cations as seen in Figure 8. Donnan exclusion causes ions with the same charge to be electrostatically repelled from one another. In the presence of polar solvents, such as water, fixed charged groups in the matrix of polymers dissociate. Since such polymeric materials have high concentrations of fixed ionic groups, electrostatic interactions of fixed charged groups with mobile ions consequently have a significant impact on counterion transport through them (Galizia et al., 2017).

Various methods have been applied to improve the characteristics of CEMs by using distinct polymer matrices and additives. These methods include polymer mixing (Avci et al., 2020), surface modification (Siekierka et al., 2023), creation of various crosslinking and functional groups (Dong et al., 2021). Targeted CEMs should be low cost and they should have high ionic conductivity, optimal hydrophilic properties, and appropriate mechanical, thermal, and electrochemical stabilities (Nazif et al., 2023b).

Since the sulfonic acid group is hydrophilic and has a propensity to form ion clusters in the membrane matrix, it is the most studied fixed ionic group for CEMs. It can dissociate over the whole pH range. Avci et al. (2020) synthesized unique CEMs using sulfonated polyethersulfone (sPES) polymer that has been specially tuned for RED applications. These membranes were prepared by solvent evaporation and phase inversion techniques. Results highlight the importance of optimizing permeability and resistance in the design of IEMs.

To satisfy the requirements for membranes requested specifically for RED applications, which are characterized by low resistance, high selectivity, affordability, and easy preparation, it is crucial to choose polymers that are both cost effective and chemically stable for modification. Therefore, hybrid membranes emerge as promising candidates for usage in RED systems for power generation. The innovative approach suggested by Zhang et al. (2017) offers an economical and novel method for preparing hybrid CEMs. In order to enhance the CEMs' characteristics, PPO based hybrid organic-organic CEMs were prepared by solvent evaporation method for RED. The highest P_d obtained by these CEMs was 0.46 W/m² in a RED test. According to this result, a 14% increase in power generation is achieved over commercial CEMs. The use of organic-organic hybrid membranes in the RED is highlighted by this study.

Nanocomposite CEMs are prepared by incorporating organic and inorganic nanoparticles into polymeric membranes to improve the polymeric membrane performance. Nanocomposite membranes



where the polymer acts as a host for inorganic nanoparticles are a useful technique to enhance the mechanical, electrical, and physical characteristics of CEMs for RED (Hosseini et al., 2018). Nazif et al. (2023a) developed nanocomposite CEMs with sulfonated PPO (sPPO) polymer and MXene ($\text{Ti}_3\text{C}_2(\text{OH})_2$) nanosheets as fillers. The sPPO polymer matrix was not delaminated or functionalized during the study. According to the results, the CEMs with a 36% sulfonation degree (DS) had good mechanical properties, excellent electrochemical performance, and high permselectivity (>90%). While preparing the CEMs, the DS was kept constant, different amounts of MXene, and different concentrations of polymer were used. The electrochemical characteristics of the synthesized CEMs were improved by the addition of MXene. The optimum membrane showed the lowest area resistance, high permselectivity, and reasonable charge density.

Similarly, Tong et al. (2016) synthesized nanocomposite CEMs from oxidized multi-walled carbon nanotubes (O-MWCNTs) mixed with sPPO. The PPO has strong chemical, thermal, and mechanical characteristics. The sPPO is obtained by adding sulfonic acid groups to PPO polymer chains via sulfonation processes and is commonly employed in the synthesis of CEMs. According to the results, it was observed that when O-MWCNT loadings increased, so did gross P_d . A 0.5 wt% of O-MWCNT used in the synthesis of CEM demonstrated superior performance in terms of IEC, fixed-charge degree, permeability, and resistivity, with a gross P_d of 0.48 W/m^2 (14% higher than commercial FKS membrane).

Surface modification of an CEM is the most studied and a very effective approach to tune membrane ion selectivity. Ion selectivity is a membrane property that may come into play at membrane solution interfaces (Luo et al., 2018). Siekierka et al. (Siekierka and Yalcinkaya, 2022) synthesized high-selective CEMs, which are subsequently used in RED to generate power while recovering cobalt cations. Employing a surface modification approach, they investigated the use of selective membranes to recover beneficial elements from battery mixtures. That research examined the potential to produce energy from battery effluents having cations such as Co, Li and Ni. The CEM was prepared by obtaining homogeneous films synthesized by dry phase inversion of polyacrylonitrile (PAN) and dimethylformamide mixture. The highest power generation was predicted as 0.44 W/m^2 , and the

separation factors for Co, Li, and Ni were 0.80, 0.14, and 0.06, respectively.

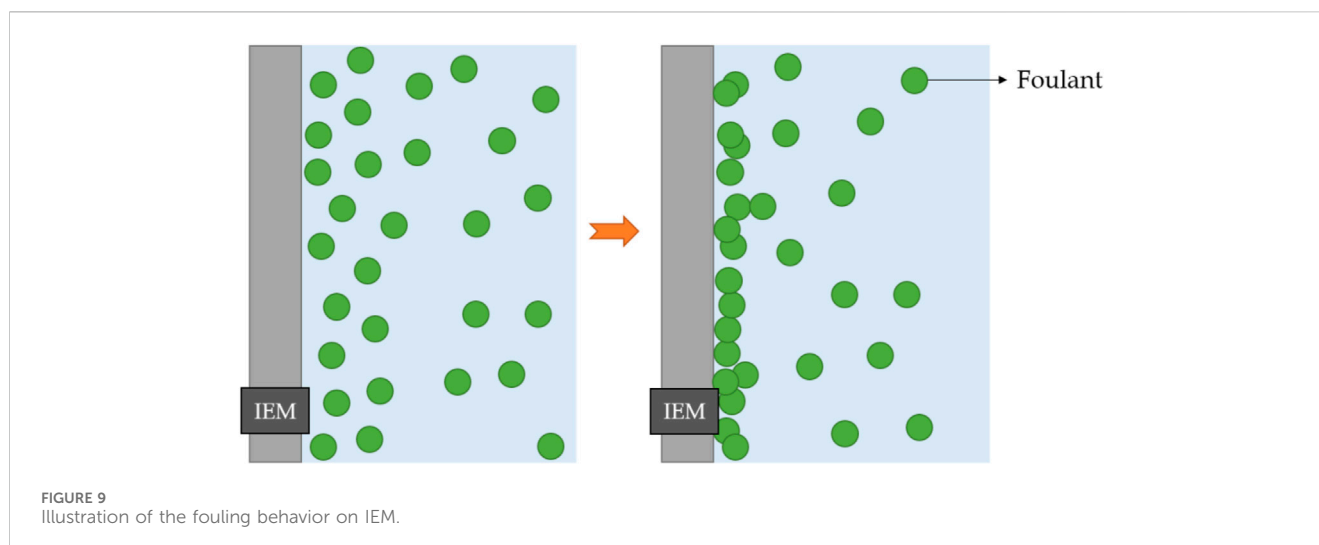
The creation of a regular polymer chain network results in improved chemical and mechanical stability of membranes when the density of crosslinking is controlled by varying the content of crosslinking functionality in polymer networks (Zhu et al., 2019). Poly (vinyl alcohol) (PVA) contains a substantial amount of reactive chemical functional groups, which can be crosslinked using thermal, irradiation or chemical treatments. Dong et al. (Dong et al., 2021) prepared specially produced PVA/SSA (sulfosuccinic acid, SSA) based CEMs for their use in treatment of wastewater or power generation systems by RED. In their studies conducted with different SSA loading amounts, the PVA/SSA based CEM containing 20% SSA by weight was preferred due to its excellent mechanical and transport properties. The thermally treated CEMs at a crosslinking temperature of 120°C exhibited optimum electrochemical properties. The RED performances of both tailored and commercial Selemion CEMs gave P_d values of 1.022 W/m^2 and 1.072 W/m^2 , respectively and their performances were considered to be similar.

Conducting polymers and chitosan (CS) based composite materials have the possibility of easy synthesis, thin film formation, and functionalization to modify material properties. In this context, Tufa et al. (2020) conducted a study to develop monovalent selective CEMs (Figure 8B). These CEMs allow limited divalent Mg^{2+} permeability across the membrane while allowing rapid transfer of Na^+ ions.

The CEMs consisting polypyrrol/chitosan (PPyCS) composites offer a strong chance of overcoming the detrimental effects of multivalent ions in RED. The measurement of OCV in RED tests with multivalent ions containing solutions shows that pyrrole (Py) polymerizes chemically on the surface of CEMs, offering a dense and tight structure that allows for the increase of the monovalent selectivity. The CEMs consisting of PPyCS composites are capable to reduce the adverse effects of multivalent ions in RED tests. On the surface of CEMs, Py chemically polymerizes to produce a tight, rigid structure that increases monovalent selectivity. For this purpose, commercial CEMs have been optimized by carefully controlling the polymerization duration, and Py and CS molar concentrations in the composite solution. The average 42.6% of

TABLE 3 Properties of AEMs and CEMs for RED applications given in the literature.

Membrane pairs		Thickness (μm)	IEC (meq/g)	Water uptake (%)	Perm-selectivity (%)	Area resistance ($\Omega\cdot\text{cm}^2$)	Salt concentration	OCV (V)	P_d (W/m ²)	Ref.
AEM	CEM									
PECH B-1	CMX (Neosepta)	33	1.68	49.0	86.5	0.82	0.017/0.513 M NaCl	-	1.27	Guler et al. (2012)
E2C1–DMA0.5–DAB	CMX (Neosepta)	25	1.39	-	93.8	0.754	0.017/0.513 M NaCl	-	1.52	Choi et al. (2018)
PErC(5)QPS-QPPO	CMV (Selemion)	51	1.20	37.0	-	0.69	0.0085/0.599 NaCl	-	1.82	Lee et al. (2019)
VBC:DMAEMA = 1.0:1/DVB0.10	CMX (Neosepta)	24	2.06	17.9	88.1	0.93	0.017/0.513 M NaCl	0.756	0.45	Song et al. (2022)
GAM-1	GCM 1	77	2.15	24.2	-	0.64	0.1/0.5 M NaCl	-	2.10	Golubenko et al. (2021)
AMX (Neosepta, Japan)	sPES-P	83	1.15	67.2	84	-	0.1/4.0 M NaCl	0.291	3.23	Avci et al. (2020)
	Spes-D	63	1.19	28.0	95			0.314	3.92	
ASE (Neosepta)	PAN	150	1.66	2.7	-	116.90	0.0001/0.1 M HCl	2.140	0.44	Siekierka et al. (2023)
AMV (Selemion)	PVA/SSA	120	1.80	29.8	90.4	2.55	0.017/0.5 M NaCl	0.703	1.02	Dong et al. (2021)
AMX (Neosepta, Japan)	sPPO MXene	25–40	2.18	42.0	91.3	1.30	0.017/0.5 M NaCl	0.182	1.45	Nazif et al., 2023b
FAS (Fumasep [®] , Germany)	PPO sPVA	50	2.00	48.0	87.2	-	0.017/0.5 M NaCl	-	0.46	Zhang et al. (2017)
FAS (Fumasep [®] Germany)	O-MWCNT sPPO	70	2.28	42.1	95.3	0.45	0.017/0.5 M NaCl	-	0.48	Tong et al. (2016)
Fuji-AEMT1 (Netherlands)	Fuji CEMT1-PPyCS	122	1.70	47.4	-	2.12	0.5/4 M (NaCl in MgCl ₂)	0.210	1.50	Tufa et al. (2020)



increase in maximum P_d that was seen for the modified membranes over the pristine membranes with the overall improvement in OCV. Table 3 indicates the features and RED performance of tailored and commercial IEMs (Tufa et al., 2020).

4 Fouling on ion exchange membranes

In real-life applications, the performance of RED system may encounter certain challenges such as membrane fouling, scaling and biofouling (Pawlowski et al., 2019). Fouling in membrane systems occurs as a result of concentration polarization, which causes a cake layer or pore blockage by organic substances (Figure 9). This polarization increases the rejected component near the membrane surface, causing damage on membrane and reducing flux. Conversely, membrane scaling happens when dissolved substances accumulate up on the membrane, decreasing flux (Othman et al., 2022a).

The fouling phenomenon causes the membrane's electrical resistance to increase and the system's P_d to decrease, which adversely impacts IEM performance and potentially increasing overall costs (Park et al., 2003; Mikhaylin and Bazinet, 2016; Pawlowski et al., 2019). The fouling of IEMs may reduce the overall performance of RED stacks, inhibiting the long-term sustainable energy production, and reduction of possibly a lower lifespan of membranes (Bodner et al., 2019; Othman et al., 2022b; Vital et al., 2023). Fouling exerts a significant impact on crucial operational parameters, notably manifesting as an elevated pressure drop, increased both ohmic resistance (R_{ohmic}) and non-ohmic resistance ($R_{non-ohmic}$), and a reduction in the OCV generated through the salinity gradient across an IEM. RED systems are susceptible to diverse forms of fouling, encompassing organic fouling (such as polysaccharides, oils, polyelectrolytes, humic acids, alginate, and sodium dodecyl sulfate), biofouling, particulates, microorganisms, inorganic fouling involving scaling (mineral precipitates such as magnesium, calcium, iron, and barium) and uphill transport of multivalent cations like Ca^{2+} and Mg^{2+} , membrane poisoning, as well as adhesion and deposition of

colloids (such as clays, flocs) (Chae et al., 2013; Bodner et al., 2019; Eti et al., 2021; Othman et al., 2022b; Vital et al., 2023).

Large negatively charged molecules are usually attracted to the surface charge of AEMs and cause organic fouling. Compared to CEMs, AEMs are more susceptible to fouling issues because of interactions between their fixed positive charge groups and negatively charged natural organic matter (Park et al., 2003). On the other hand, scaling in RED systems tends to be more prevalent with CEMs, influenced by both morphological and electrochemical properties. Spacers, deemed more susceptible to biofouling than membranes, play a crucial role in membrane fouling (Eti et al., 2021).

A notable investigation conducted by Vermaas et al. (Vermaas et al., 2013) delved into fouling issues within RED stacks over a 25-day of operational span without cleaning, using authentic sea and river water as feed. The findings indicated, a three-point surge in pressure drop and a substantial 60% decline in P_d for 25 days, under these untreated circumstances. The study highlighted the significant impact of membrane charge on the rate and fouling nature. Specifically, the AEM exhibited traces of diatoms, clay minerals, and organic substances, whereas the CEM displayed inorganic species such as calcium phosphate desquamation.

Santoro et al. (2021) explored fouling effects on RED performance using seawater and hypersaline brine. Fujifilm's IEMs are examined for fouling susceptibility. As a similar outcome, theoretical modeling, validated by $CaCO_3$ precipitation, indicates CEM vulnerability to scaling. FTIR-ATR analysis reveals AEM sensitivity to organic fouling. Laboratory-scale RED tests with artificial seawater and brine exhibit increased pressure drop, 23% reduction in gross P_d , and negative net P_d .

According to a study conducted by Han and Park (2021), the following conclusion has been drawn that systematically classified surfactants into three groups: negatively charged, positively charged, and non charged, based on molecular weight to minimize macromolecule interaction between IEMs and surfactants. The objective of that study was to understand the way each type of fouling acts in a RED system, taking into account elements such as electromigration, adsorption, electrostatic attraction, and macromolecule interaction. Surprisingly, despite expectations, the

worst fouling tendency occurred in river freshwater with charged foulants rather than in seawater. Zeta potential measurements indicated that the RED system's fouling tendency decreased as a result of a reduction in Debye length caused by the higher ionic strength of seawater streams. The research emphasized the importance of considering both non charged and charged foulants present in natural freshwater and seawater streams in RED systems, emphasizing the need for fouling resistance strategies and antifouling methods.

In the context of natural waters, mitigating membrane fouling in RED systems can be achieved through pretreatment methods or by incorporating a tailored membrane design (Hong et al., 2015). To address fouling concerns, the development of highly selective AEMs without increasing electro-resistance is essential. Various surface modification techniques, including graft polymerization, dip coating/immersion, electrodeposition, layer-by-layer deposition, plasma treatments, and solution casting, can be applied to control fouling and enhance AEM performance (Eti et al., 2021). Specifically, adding a charged coating layer containing polyelectrolyte to the membrane structure may enhance its antifouling and monovalent ion selectivity (Hong et al., 2015).

Gao et al. (2018) introduced a layer-by-layer deposition method for AEMs, resulting in a modified AEM labeled CJMA-2-7.5, demonstrating monovalent anion selectivity and antifouling properties by the CJMA-2-7.5 membrane outperformed the commercial ACS membrane and the standard CJMA-2 membrane by 38.43% and 30.29%, respectively, in terms of its ability to resist organic fouling.

Guler et al. (2014) coated a commercial membrane to design monovalent selective AEMs, using 2-acryloylamido-2-methyl propane sulfonic acid and N, N-methylene bis (acrylamide) for the coating layer. Although the modified membranes exhibited increased hydrophilicity (contact angle decreased from 63.6° to 23°), monovalent ion selectivity, and antifouling characteristics, they were less effective in achieving higher power densities in RED.

Using zwitterionic materials is one of the innovative methods used to avoid fouling during the application of AEMs for a long period of time in RED applications. Since zwitterionic materials have both positive and negative charged groups, they are more hydrophilic and have lower adhesion, which helps to prevent fouling in RED applications when used for extended periods of time (Kotoka et al., 2020; Pintossi et al., 2021). Pintossi et al. (Pintossi et al., 2021) aimed to prevent fouling issues on AEMs within the RED system. They produced antifouling membranes through surface modification using a commercial AEMs, Fujifilm AEM type I. The surfaces were modified using zwitterionic layers, and their antifouling properties were evaluated. They employed two different methods for modification. First, by depositing a polydopamine layer using zwitterionic monomers, followed by surface grafting through a reaction with sulfobetaine, second, by modifying polydopamine onto a zwitterionic brush-modified surface, followed by the accumulation of polysulfobetaine through atom transfer radical polymerization. These changes led to an increase in the hydrophilicity of the membrane due to the zwitterionic layers. The antifouling behavior in RED was assessed using artificial river and seawater. While zwitterionic monomers delayed the onset of fouling, they almost did not affect the accumulation of fouling layers. However, membranes modified

with zwitterionic brushes resulted in higher P_d outputs by delaying the onset of fouling and slowing down the growth of fouling layers. While unmodified AEMs lost 65% of their initial gross P_d , membranes containing zwitterionic monomers and brushes lost 60% and 52%, respectively. Zwitterionic modifications increased the membranes' hydrophilicity and reduced their contact angle with water.

One of the surface modification techniques to prevent fouling is dip coating. This method involves immersing a membrane in a solution containing a modifying agent for a specified duration, serves to establish an additional layer with desired properties (Khoiruddin et al., 2017). Tiago et al. (2022) coated commercial polyester based heterogeneous Ralex membranes with a more environmentally friendly chemical, polyacrylic acid, using the dip coating method. Subsequently, they evaluated the fouling performance of commercial AEMs by employing seawater and surface water containing *Aeromonas hydrophilia*, which is commonly found in various aquatic environments and frequently forms biofilms. They then used model organic foulants such as sodium dodecyl sulfate and sodium dodecyl benzene sulfonate (SDBS). Furthermore, they assessed and compared the effects of chemical cleaning with sodium hydroxide and sodium hypochlorite solutions on fouled membranes. The modified AEMs exhibited lower fouling characteristics compared to unmodified ones, while also enhancing monovalent permselectivity. Following (bio)fouling events using natural feed waters, the use of sodium hypochlorite as a chemical cleaning solution revealed an efficient restoration of initial membrane properties. This finding holds great importance for improving the efficiency of RED processes.

As advancements progress, the potential for RED to become a viable and effective sustainable energy source in the future is high due to its ability to obtain energy from salinity gradients. Improving the stack's electrochemical characteristics and optimizing spacer design, electrode demands, energy consumption of pumping, and water pretreatment to minimize fouling are all necessary to ensure the technology's successful development (Vermaas et al., 2013).

Bodner et al. (2019) conducted studies using a crossflow RED stack divided into half stacks for the configuration of the RED fouling monitor providing a comprehensive precise, and instantaneous analysis of fouling for RED application. Each half stack facilitated either the oxidation reaction at the anode or the reduction reaction at the cathode, utilizing platinum coated titanium electrodes and a homemade dynamic flow through salt bridge for ionic connection. The continuous renewal of the electrolyte solution and independent reference electrodes ensured stable operation, allowing simultaneous monitoring of fouling. The introduced RED fouling monitor is highlighted as an innovative tool for comprehensive fouling analysis in RED. Investigating its practical utility under both unfouled and organically fouled conditions, particularly with SDBS, the study reveals diverse fouling behaviors, emphasizing the intricate nature of fouling in RED systems. The findings underscore the complexity of fouling in RED and stress the necessity of thorough studies employing the RED fouling monitor. This versatile tool efficiently distinguishes and categorizes RED fouling, providing insights into the impact of IEMs exposed to specific feeds. With a functional design involving a flow through salt bridge and closely positioned reference electrodes, it demonstrates stable operation under clean conditions. The monitor

tracks the time dependent progression of relevant fouling parameters, offering insights under both OCV and current conditions. Additionally, it provides valuable information on the effects of current density and field direction on fouling behavior, offering unique perspectives into R_{ohmic} and $R_{non-ohmic}$. The concept is extendable to other IEM based systems prone to fouling, and its versatility extends to specific analyses of IEM coupons for various applications, including systematic fouling studies, pretreatment testing, environmentally friendly cleaning techniques, and exploring the fouling potential of different feed streams. The monitor's sensitivity makes it a useful tool for early fouling detection or as a warning system (Bodner et al., 2019).

In RED systems, various fouling removal methods are available, including mechanical cleaning and chemical treatments. Mechanical cleaning stands out as a sustainable practice compared to chemical cleaning because it involves adjusting operational parameters, while chemical cleaning poses risks to membrane structure and generates toxic byproducts (Vital et al., 2023). Vital et al. (2023) focused on fractionating seawater foulants and assessing fouling reversibility using environmentally friendly cleaning methods. Different techniques, such as alternating seawater and fresh water, reversing inlet and outlet, and chemical cleaning, were investigated, with periodic air sparging showing superior performance despite higher energy consumption. Techniques like flow reversal and a three-step process successfully reversed 60% of pressure drop increase in stacks fed with dual media filtered seawater over 2 months. A dual media filter for seawater pre-treatment, combined with a chemical free cleaning procedure, demonstrated the sustainability of blue energy technology, recovering 90% of performance loss. The findings offer insightful information for the advancement of IEM technologies and environmentally friendly energy solutions in the future.

The introduction of natural water that contains multivalent ions causes inorganic scaling to occur around the cathode and inside the membrane stack due to ion crossing through the protective membrane. The interaction with hydroxide ions created during water reduction is the cause of this. Han et al. (Han et al., 2019) suggested using a bipolar membrane (BPM) as a protective membrane at the cathode to inhibit inorganic precipitation as a way to mitigate this problem. The bilayer structure of the BPM, involved in water splitting, effectively hinders ions from diffusing from the catholyte and the feed solution, thereby maintaining current density. In order to decrease inorganic scaling near the cathode in a RED system, they used a BPM in their study, which demonstrated to be the most effective in preventing the production of precipitates. As a result, it can be employed to create an extremely stable electrode system for a large-scale RED system that uses natural water to operate for an extended period of time. In the context of RED utilizing a BPM positioned at the cathode, the objective is to mitigate inorganic scaling caused by water reduction and the presence of multivalent cations in a natural feed solution. The configuration involves directing the cation exchange layer and anion exchange layer of the BPM towards the feed solution and catholyte, respectively. This specific orientation enables the BPM to experience water splitting when it is subjected to a forward bias that is induced by the RED system's stack voltage. The water splitting

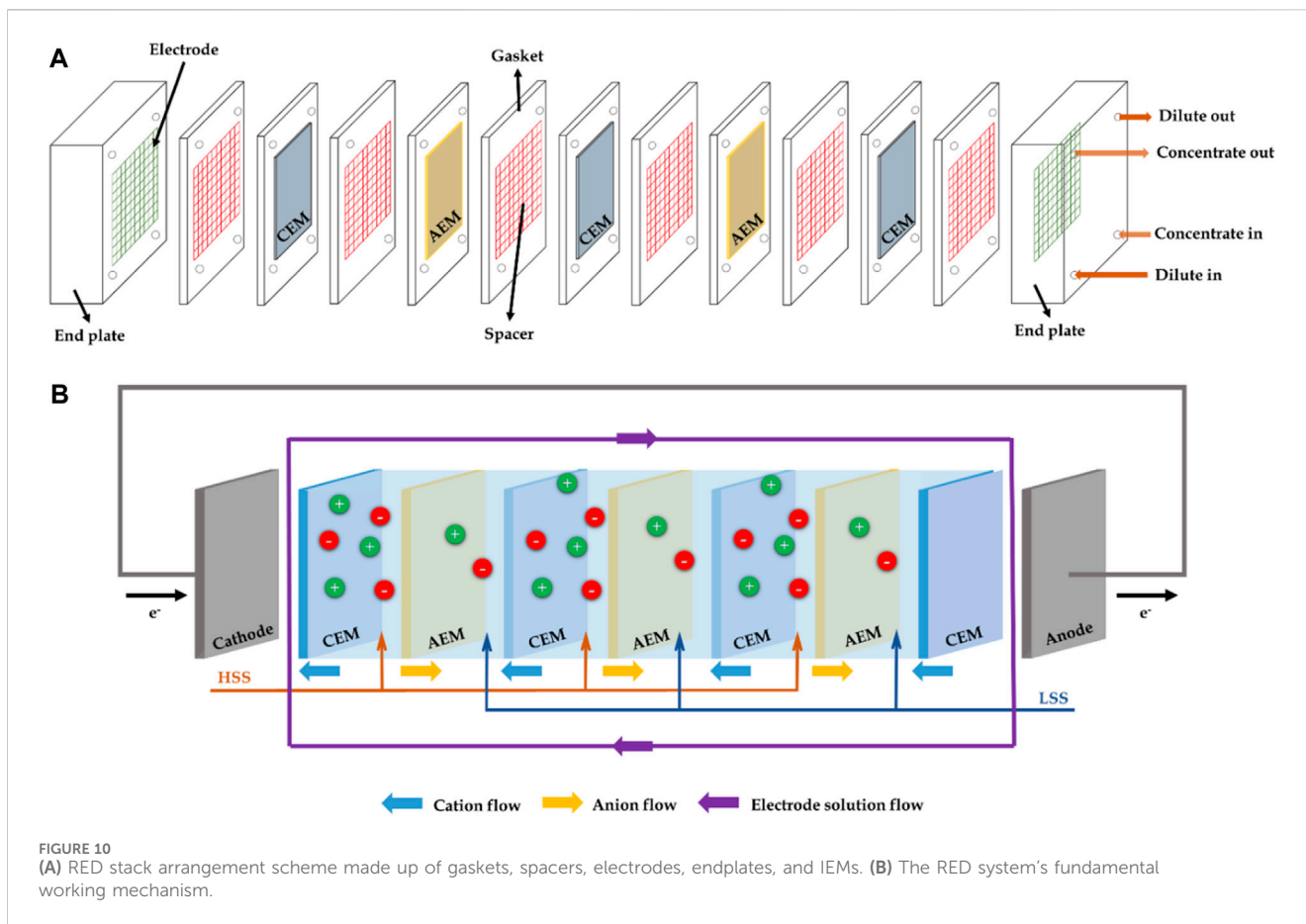
occurring within the bilayer of the BPM plays a crucial role in preventing the crossover of hydroxide ions and multivalent ions, thereby addressing the issue of inorganic scaling.

Jwa et al. (2023) study investigated inorganic fouling in seawater based electrochemical devices, focusing on cathodic electrocatalysts for large-scale RED. Nano-Pt/C shows superior scaling control over bulk Pt, forming a thin and porous $Mg(OH)_2$ layer. Strong anti-fouling behavior at high voltages is exhibited by surface-modified carbon nanostructures, especially O-rich functionalized C catalysts treated with acid air plasma, which leads to stable RED performance. The control of inorganic scaling behaviors is explored using various Pt- and/or C-based cathodic electrocatalysts in both artificial solution and real seawater. Nano Pt/CB/CC (CB: carbon black, CC: carbon cloth) demonstrates better scaling control than bulk Pt, and O-rich functionalized CBs show the best anti-scaling behavior.

5 Recent developments in RED stack design and applications

The main component of a RED process is so-called a RED stack. The stack, as shown in Figure 10A, mainly composes of endplates, electrodes (anode and cathode), AEMs and CEMs stacked in an alternating pattern, and spacer/gasket separating IEMs from each other. Two solutions with different salinities, high concentration salt solution (HCS) and low concentration salt solution (LCS), are alternately fed to the stack. The anions and cations in the solutions permeates through the membranes, creating a potential difference between the electrodes. Simultaneously, the electrode solution is circulated in the electrode cells continuously. The electrodes use the potential energy created in the cell to carry out the oxidation and reduction reactions, which then is converted to electrical current (Figure 10B) (Jeong et al., 2021). The selection of electrodes significantly affects power generation efficiency by influencing factors such as voltage loss, thermodynamic potential, and concentration polarization (Jang et al., 2020). Structural and compositional modifications of electrodes can enhance the power generation capacity and durability of RED systems. For example, modifications like platinum coating on titanium-based electrodes can improve electrochemical performance by increasing surface area and reducing resistance, thereby enhancing system efficiency (Jeong et al., 2021).

The design and electrode materials selection of electrodes used in RED systems depends on the application scale, such as laboratory or industrial. For instance, inert electrodes are common in laboratory-scale systems, whereas specially designed electrodes are used for industrial-scale systems (Jang et al., 2020). Redox solutions commonly used at the laboratory scale (e.g., hexacyanoferrate) are contentious for large-scale applications in terms of sustainability, stability, and economic viability (Simões et al., 2023). In large-scale systems, choosing the right electrode system is vital for optimizing long-term stability and operational costs (Jang et al., 2020). Asymmetric electrode systems are proposed for achieving stable operation in large-scale RED systems. Particularly in systems where the geometric area of the cathode is smaller than that of the anode, asymmetric electrode systems can reduce power loss and stabilize electrode reactions. These systems



provide avenues for research and development to support the economic and sustainable applications of RED (Han et al., 2020).

On the other hand, alternative electrode systems such as carbon-based flow electrodes offer advantages such as low cost, ease of scalability, and environmental compatibility for large-scale RED applications. These electrodes rely on the electrostatic double-layer adsorption of ions on carbon surfaces and do not require faradaic redox reactions. However, after adsorption saturation, reversing polarity may be necessary for desorption, leading to an intermittent charge and discharge process. Research emphasizing the importance of enhancing electrode conductivity through studies on the improved performance of carbon-based flow electrodes, including the addition of conductive additives like carbon black, underscores their utility (Simões et al., 2023).

The overall electromotive force created in RED, which is the sum of the Nernst potential across each cell, is the OCV, theoretically obtained using the Nernst equation:

$$OCV = \frac{NRT}{F} \left[\frac{\alpha_{CEM}}{z_+} \ln \frac{\gamma_c c_c}{\gamma_d c_d} + \frac{\alpha_{AEM}}{z_-} \ln \frac{\gamma_c c_c}{\gamma_d c_d} \right]$$

Where α is the IEM's permselectivity, N is the number of membrane pairs (cell pairs), R is the gas constant, T (K) is the temperature, F is the Faraday constant, z is the charge of the ions, c is the molar concentration, γ is the activity coefficient, subscripts c and d represent concentrated and dilute, respectively. The R_{ohmic} , the $R_{non-ohmic}$ and the electrode system resistance make up the internal

stack resistance (R_i) in RED. The resistance of the feed compartments and the IEMs account for a great deal of the R_{ohmic} inside the stack caused by ionic transport limits via the stack components. Diffusion boundary layer resistance (R_{DBL}) and electrical double layer resistance (R_{EDL}) are attributed to the $R_{non-ohmic}$ (Tufa et al., 2018).

$$R_i = R_{ohmic} + R_{EDL} + R_{DBL}$$

The performance of a RED stack is evaluated by calculating the net power density, which is mathematically represented by the following equation:

$$P_{net} = P_{gross} - P_{pump}$$

$$P_{gross} = \frac{OCV^2}{4 \times R_i}$$

$$P_{pump} = \frac{2 \times \Delta p \times q}{L}$$

where P_{gross} is the gross power density, P_{pump} is the power used by the pumps, OCV is the open circuit voltage, R_i is the total internal resistance, Δp is the pressure drop over the inlet and the outlet, q is the flow rate per cell per unit width, and L is the unit length (Vermaas et al., 2011a).

Resistances play an important role in RED design as they affect P_d . The resistances in RED can be divided into two subgroups R_{ohmic} is obtained as a result of the ionic transport through individual components such as IEMs, spacers, and HCS and LCS. On the other

hand, $R_{\text{non-ohmic}}$ is induced by a reduction in the concentration gradient between solutions with HCS and LCS, which decreases the electromotive force generated. $R_{\text{non-ohmic}}$ can be divided into two types: R_{DBL} , also known as concentration polarization, and R_{DAC} , caused by the concentration changes in the bulk solution (Dong et al., 2020).

5.1 Spacers

Spacers are employed in various membrane-based processes, serving as spacer filled channels in electrodialysis and spiral wound modules for reverse osmosis, among various other applications. In these instances, the geometry of the spacers, encompassing factors like filament thickness, distance, and angles, is consistently recognized as crucial for influencing performance of process parameters such as mass transfer, pressure drop and resistance (Vermaas et al., 2014; Mehdizadeh et al., 2019).

Spacers in RED are essential elements, mainly used to create spacing between the membranes to allow the tortuous flow between these membranes. However, on the whole, the flow path is a function of spacer filament dimensions. In order to improve turbulence near the IEMs without the use of traditional mesh or filament spacers and to increase mass transport without raising the pressure drop in the RED stack, there is a room to investigate various flow patterns in the flow path or cavity. Typically, this involves arranging mesh and filament spacers in various designs (Basu and Mahajan, 2023).

Basu and Mahajan (2023) developed a new cavity type flow channel that may be used in the place of conventional spacers in order to improve the performance of the RED stack. This study's methodology is based on the computational fluid dynamics (CFD) examination of flow paths with various configurations and designs. For design and analysis, three-dimensional Direct Numerical Simulation of the transient Navier-Stokes equations is performed using standard spacers. The pressure drop and shear stress simulation results for various flow path designs are compared, and the flow characteristics are examined and discussed. In comparison to other designs, it is discovered that the diamond patterned flow field offers a higher and more uniform distribution of shear stress. The diamond design also exhibits a lower pressure drop per unit length and a comparable range of shear stress when compared to mesh spacers. It is suggested that the diamond spacer design could enhance RED performance by reducing concentration polarization loss.

The spacers used in RED are classified as either conductive or non-conductive. Longer pathways are created for the transport of ions in solutions by non-conductive spacers, which partially cover the membrane surface. The R_{ohmic} may nearly double as a result of this "spacer shadow effect" (SSE) (Tufa et al., 2018). The RED system's power output is significantly reduced as a result of the SSE, as well as increases R_i (Li et al., 2024).

The prediction of SSE in a single cell pair resistance (R_{CP}) has been investigated and following general relationship is obtained:

$$R_{\text{CP}} = \beta_{\text{sol}}(R_{\text{sea}} + R_{\text{river}}) + \beta_{\text{mem}}(R_{\text{AEM}} + R_{\text{CEM}})$$

where β_{sol} and β_{mem} are the coefficients to express the SSE on solution compartment and membrane, respectively (Mehdizadeh et al., 2019).

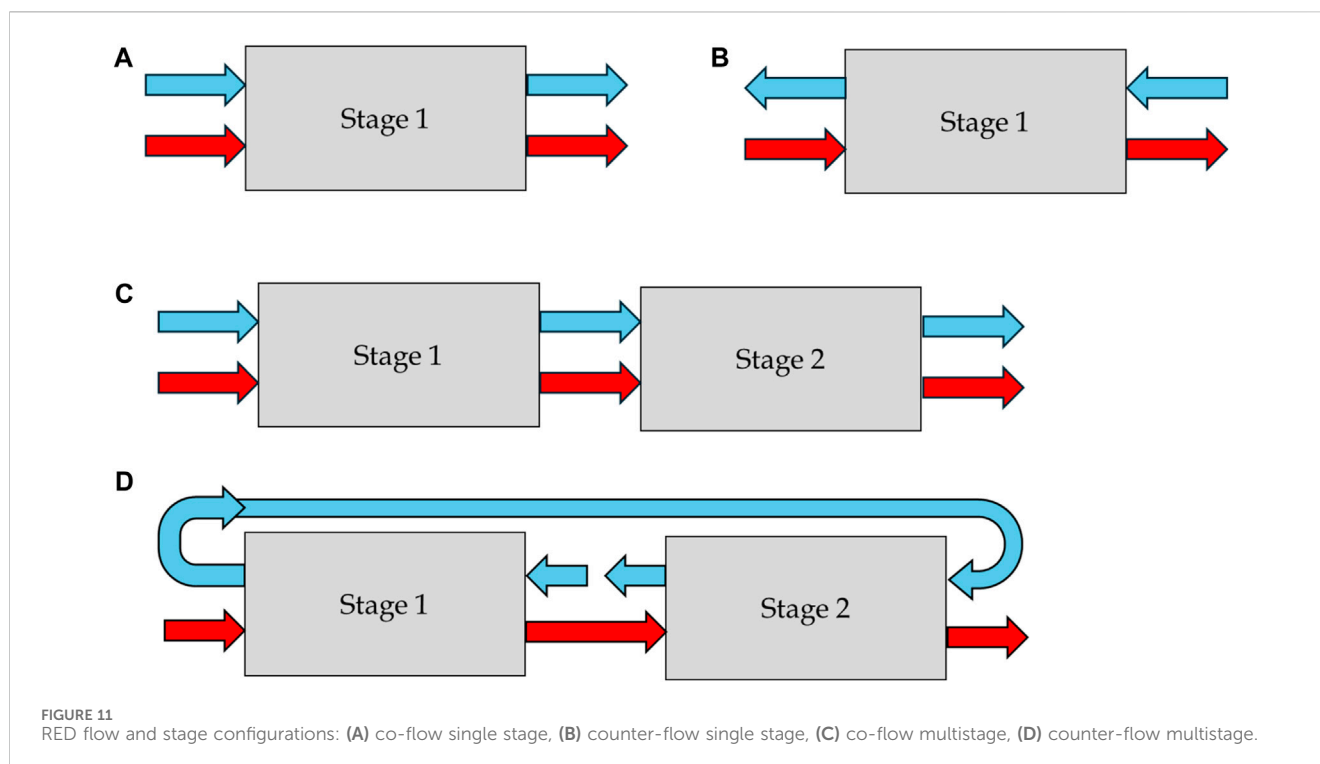
Post et al. (2008) investigated both parameters separately. They searched for suitable dimensional parameters of the spacers correlating with only β_{sol} , and they proposed that the parameter was inversely proportional to the square of the porosity of the spacer ($1/\epsilon^2$). Mehdizadeh et al. (2019) conducted an in-depth examination on the prediction of the SSE. They investigated sixteen different spacers and proposed new parameters for predicting the SSE that are connected to the geometric properties of the spacers. The results indicated that there is a strong correlation between the SSE on a membrane and a parameter that includes both the area fraction and diameter of spacer filaments.

Commercial spacers which are non-conductive and made from industrial materials like nylon, PE, and polytetrafluoroethylene often cover the IEMs' effective area and decrease ionic conductivity (Li et al., 2024). One of the major drawbacks of using a non-conductive spacer for RED is the increased resistance, which is related to spacer thickness. Vermaas et al. (2011a) investigated the effect of spacer thickness on the RED performance. Spacers with thicknesses of 485, 200, 100, and 60 μm were utilized, and it was found that the best result was achieved with the 100 μm spacer. The reason the 100 μm spacer outperformed compared to the 60 μm spacer is attributed to the observation that below a certain thickness, $R_{\text{non-ohmic}}$ increases, leading to a decline in performance (Vermaas et al., 2011a; Kim et al., 2015; Mehdizadeh et al., 2019).

Although non-conductive spacers are commonly employed in RED studies, investigating ion-conductive spacers and profiled membranes as a substitute presents a unique strategy for improving the performance of RED. Ion conductive spacers enable ion transport through membrane sites that are otherwise blocked by the spacers. This prevents the SSE and enhances performance significantly. Długolecki et al. (Długolecki et al., 2010) studied the impact of ion conductive spacers on the performance of the RED stack. They used different spacers with the same open area. Ion conductive spacers had two parts, one for anion transfer, and one for cation transfer, and were always placed between an AEM and a CEM. They found that ion-conductive spacers increased P_d output by a factor of three to four while decreasing R_i by a factor of two compared to the non-conductive spacers.

Profiled membranes are an alternative to spacers in RED since they create a channel for fluid flow while separating two adjacent membranes through reliefs on their surface. When profiled membranes are used instead of non-conductive spacers, a higher power output can be achieved in RED. The main cause of the observed improved performance is the decrease in R_{ohmic} brought about by the removal of the SSE (Tufa et al., 2018). In comparison to a stack with spacers, Vermaas et al. (2011b) achieved a 10% higher net P_d using profiled membranes with straight ridges oriented parallel to the direction of fluid flow.

Nevertheless, poor fluid mixing and stagnant flow are two issues with the single-sided profiled membranes that are currently in use. The precise assembly of stacks and membrane preparation for double sided profiled membranes remain challenging. Dong et al. (2020) considering these issues, suggested a single sided wavy profiled membrane with wavy sub corrugations as an additional mixing promoter. The wavy sub corrugations added to the ridge structured membrane in this profiled membrane served as extra mixing promoters. The properties of mass transfer and



hydrodynamics were evaluated by means of CFD simulation through comparisons with the woven spacer channel and several other profiled membrane channels. The wavy profiled membrane was found to have a lower concentration polarization factor and a higher mass transfer coefficient when compared to square and circular pillar profiled membranes. However, both the woven spacer channel and the double sided chevron profiled membrane outperform the single-sided wavy-profiled membrane. The study suggests that increasing the width and height of the sub corrugations and decreasing the straight ridge spacing can enhance mass transfer performance in the wavy profiled membrane channel.

In the literature, studies have primarily focused on suppressing the shadow effect by substituting nonpermselective spacers with profiled membranes and lowering R_i by varying the geometry and arrangement of profiled membranes. However, ion transport across the membrane is limited because of the low permeability of profiled membranes. Thereby, the shadow effect remains serious. Moreover, the conductivity of profiled membranes is low induced by the use of heterogeneous membrane materials, and then the RED system still has a higher R_i and lower P_d . Therefore, it is urgent to explore a novel spacer design to inhibit the shadow effect for obtaining lower R_i and higher P_d (Li et al., 2024).

Li et al. (2024) proposed a design using ion permselective woven mesh spacer to reduce the SSE. Subsequently, they compared the effects of the proposed design on R_i , OCV, and P_d among nonpermselective, permselective, and permselective woven mesh spacers. Ion permselective woven mesh and silicone gasket are the components of an ion permselective woven mesh spacer. Anion and cation woven strips alternate in the permselective woven mesh. The position of the cation strips made of CEM materials is vertical, and the anion strips made of AEM materials are horizontal. In comparison to conventional spacers, this study has demonstrated

that ion permselective woven mesh spacers effectively inhibit SSE by 90%. A higher P_d is harvested due to a significant decrease in R_i caused by the elimination of the SSE. The resistance drops by 27.3% and the maximum P_d of the stack is enhanced by 45.3%. In contrast to permselective spacers, permselective woven net spacers boost P_d by up to 11% because of their larger turbulence impact, which results in less concentration polarization.

5.2 Flow modes and stage configurations

RED performance can be enhanced using various flow modes and stage configurations (Figure 11). Multistage RED is a technology that offers significant advantages over single-stage systems. Multistage RED stands out for its ability to optimize process conditions through independent electrical control of each stage. This feature allows for the application of different currents to each electrode pair, thereby increasing power output and optimizing energy efficiency (Simões et al., 2021). Moreover, the flexibility to adjust stages with different configurations and materials can further enhance performance (Simões et al., 2022). Therefore, multistage RED systems can efficiently utilize water sources derived from high salinity environments. Veerman et al. first established the multistage RED concept as a cascade operation; compared to a single stage stack, a three stage RED system enhanced its energy efficiency by more than 50% (Wang et al., 2024).

Wang et al. (2024) provide an improved mathematical model for a multistage RED system based on a series control method. Changes in density and volumetric flow rate dependent on concentration along the flow direction are considered in this model. The optimal conditions for highest power output under different series stages and sources of salinity gradient are found using Particle Swarm

Optimization. When compared to a single-stage RED stack, the multistage RED system with series control provides significantly more power output and energy efficiency. The findings indicate that the net power output and energy efficiency initially increase with the number of stages, reach their maximum values, and then decrease. With increasing feed solution concentrations, the optimal number of stages for maximum net power increases. An optimal net power output of 4.98 kW is reached for 5 M/0.05 M solutions at 12 stages, and 2.04 kW net power output is reached for 2 M/0.05 M solutions at seven stages.

Simões et al (2022) examined the performance of a two-stage cross-flow RED system that was fed with river water (Lake IJssel, $0.52 \pm 0.02 \text{ m}\cdot\text{cm}^{-1}$) and natural seawater (Wadden Sea, $31.4 \pm 4.1 \text{ m}\cdot\text{cm}^{-1}$) for a period of more than 30 days. The energy efficiency values were between 30% and 37%, and the gross power density varied between 0.3 and 0.4 W m^{-2} . Even in the presence of low salinity gradients during the test period, the two stage series configuration of multistage RED was shown in this study to be an appropriate configuration for improving energy efficiency with a consistent gross power density.

In terms of flow modes, generally counter-flow operation is more effective and produces a more uniform driving force throughout the device. However, co-flow operations might be useful in some circumstances based on flow rates. For instance, Veerman et al. (Tufa et al., 2018) discovered that due to the fact there were less local pressure differences between the river water and seawater, co-flow operation had a slightly greater P_d than counter-flow operation.

On the other hand, Gao et al. (2023) investigated the impact of flow modes on the SGE harvesting performance of the RED between concentrated brine and seawater, models taking flow modes into account were built. The models were used to analyze how feed parameters and stack sizes under two flow modes affected the RED performance. The findings show that, in both single and multi stage RED stacks, the counter-current mode performs better than the co-current. When the number of stages is 10, the energy conversion efficiency of multistage RED stacks in the counter-current mode is 5.4% higher than the co-current mode, as is the maximum net power density, which is also 6.1% higher. Therefore, when utilizing RED technology to capture the SGE between concentrated brine and seawater, it is recommended that the feed solution is in the counter-current mode. In counter-current mode, feed parameters generally exhibit better performance with higher concentrations of concentrated solution, higher temperatures of feed solution, and lower flow velocities. The dimensions of the RED stack are also crucial; thinner solution compartments or longer electrode plates can lead to higher energy conversion efficiency in counter-current mode.

6 Conclusion

In summary, this review paper delves into the recent advancements in IEMs, fouling issue and stack/process design for RED studies. Key highlights include the focus on enhancing the performance of AEMs—a critical component of RED systems. By investigating synthesis conditions, surface modification techniques, and commercial AEMs, researchers have paved the way for tailor-made AEMs specifically designed for RED applications. Notably, the

study confirms that pore-filled AEMs with optimal properties can be effectively employed in RED systems. Additionally, the review underscores the promise of MMMs-heterogeneous membranes that blend inorganic nanoparticles and organic polymers to achieve specific membrane structures. Techniques such as induced surface graft polymerization via UV radiation and nanocomposite membranes further enhance the mechanical, electrical, and physical characteristics of CEMs to be used for RED. However, membrane fouling remains a challenge, impacting IEM performance and overall costs. Strategies to mitigate fouling, including tailored membrane designs and pretreatment methods, are crucial for sustainable energy production in RED systems. On the other hand, the design of the stack, including spacers and operational modes, is crucial for enhancing mass transport in RED, ultimately leading to promising power output performance. The development and optimization of electrode systems can enhance the efficiency of RED systems and strengthen their commercial viability. Future research can focus on further enhancing and improving electrodes to facilitate broader adoption of RED systems at larger scales.

RED technology holds promise as a significant player in the renewable energy market. While it may not generate massive energy quantities, its true strength lies in synergistic applications alongside processes like energy conversion, storage, wastewater treatment, and desalination. Researchers will likely continue to explore this integration potential in the coming years. To make RED economically viable, cost-effective membrane design is crucial. Additionally, dedicated pilot projects and extensive global research efforts will propel RED toward greater viability as a renewable energy source.

Author contributions

TG: Conceptualization, Investigation, Writing—original draft. MA: Conceptualization, Investigation, Writing—original draft. ED: Conceptualization, Investigation, Writing—original draft. AB: Conceptualization, Investigation, Writing—original draft. AC: Conceptualization, Investigation, Methodology, Supervision, Writing—review and editing. EG: Conceptualization, Funding acquisition, Methodology, Project administration, Writing—review and editing. NK: Conceptualization, Funding acquisition, Project administration, Supervision, Writing—review and editing.

Funding

The author(s) declare that financial support was received for the research, authorship, and/or publication of this article. The authors acknowledge the financial support of TÜBİTAK through the bilateral collaboration programmes (TÜBİTAK-NCBR-2549 and TÜBİTAK-JSPS-2544; Projects Numbers: TÜBİTAK 117M023 and TÜBİTAK 221N334, respectively), EIG CONCERT-Japan project (Project Number: TÜBİTAK 118M804). A. Cihanoğlu would like to thank the financial support of TÜBİTAK through the National Postdoc project (Project Number: 118C549).

Conflict of interest

The authors declare that the research was conducted in the absence of any commercial or financial relationships that could be construed as a potential conflict of interest.

The authors AC, EG, and NK declared that they were an editorial board member of *Frontiers*, at the time of submission. This had no impact on the peer review process and the final decision.

References

- Archer, C. L., and Jacobson, M. Z. (2005). Evaluation of global wind power. *J. Geophys. Res.* 110 (D12). doi:10.1029/2004JD005462
- Avci, A., Rijnaarts, T., Fontana, E., Profio, G., Vankelecom, I., Vos, W., et al. (2020). Sulfonated polyethersulfone based cation exchange membranes for reverse electro dialysis under high salinity gradients. *J. Membr. Sci.* 595, 117585. doi:10.1016/j.memsci.2019.117585
- Bance-Soualhi, R., Choolaei, M., Franklin, S. A., Willson, T. R., Lee, J., Whelligan, D. K., et al. (2021). Radiation-grafted anion-exchange membranes for reverse electro dialysis: a comparison of *n,n,n',n'*-tetramethylhexane-1,6-diamine crosslinking (amination stage) and divinylbenzene crosslinking (grafting stage). *J. Mater. Chem. A* 9 (38), 22025–22038. doi:10.1039/d1ta05166k
- Basu, S., and Mahajan, C. (2023). Novel design of flow path spacers for reverse electro dialysis cell. *Can. J. Chem. Eng.* 101 (11), 6215–6226. doi:10.1002/cjce.24936
- Bodner, E. J., Saakes, M., Sleutels, T., Buisman, C. J. N., and Hamelers, H. V. M. (2019). The RED fouling monitor: a novel tool for fouling analysis. *J. Membr. Sci.* 570–571, 294–302. doi:10.1016/j.memsci.2018.10.059
- Chae, S., Kim, H., Hong, J. G., Jang, J., Higa, M., Pishnamazi, M., et al. (2013). Clean power generation from salinity gradient using reverse electro dialysis technologies: recent advances, bottlenecks, and future direction. *Chem. Eng. J.* 452, 139482. doi:10.1016/j.cej.2022.139482
- Choi, J., Yang, S., Jeong, N. J., Kim, H., and Kim, W. S. (2018). Fabrication of an anion-exchange membrane by pore-filling using catechol-1,4-diazabicyclo-[2,2,2] octane coating and its application to reverse electro dialysis. *Langmuir* 34 (37), 10837–10846. doi:10.1021/acs.langmuir.8b01666
- Dambhare, M. V., Butey, B., and Moharil, S. V. (2021). Solar photovoltaic technology: a review of different types of solar cells and its future trends. *J. Phys. Conf. Ser.* 1913, 012053. doi:10.1088/1742-6596/1913/1/012053
- Deng, J., Wang, L., Liu, L., and Yang, W. (2009). Developments and new applications of UV-induced surface graft polymerizations. *Prog. Polym. Sci.* 34 (2), 156–193. doi:10.1016/j.progpolymsci.2008.06.002
- Długolecki, P., Dąbrowska, J., Nijmeijer, K., and Wessling, M. (2010). Ion conductive spacers for increased power generation in reverse electro dialysis. *J. Membr. Sci.* 347, 101–107. doi:10.1016/j.memsci.2009.10.011
- Dong, F., Jin, D., Xu, S., Xu, L., Wu, X., Wang, P., et al. (2020). Numerical simulation of flow and mass transfer in profiled membrane channels for reverse electro dialysis. *Chem. Eng. Res. Des.* 157, 77–91. doi:10.1016/j.cherd.2020.02.025
- Dong, F., Xu, S., Wu, X., Jin, D., Wang, P., Wu, D., et al. (2021). Crosslinked poly(vinyl alcohol)sulfosuccinic acid (PVA/SSA) as cation exchange membranes for reverse electro dialysis. *Sep. Purif. Technol.* 267, 118629. doi:10.1016/j.seppur.2021.118629
- Eti, M., Othman, N. H., Guler, E., and Kabay, N. (2021). Ion exchange membranes for reverse electro dialysis (RED) applications - recent developments. *J. Membr. Sci. Res.* 7 (4), 260–267. doi:10.22079/JMSR.2021.534937.1482
- Fan, H., Huang, Y., and Yip, N. Y. (2020). Advancing the conductivity permselectivity tradeoff of electro dialysis ion-exchange membranes with sulfonated CNT nanocomposites. *J. Membr. Sci.* 610, 118259. doi:10.1016/j.memsci.2020.118259
- Faraj, M., Boccia, M., Miller, H., Martini, F., Borsacchi, S., Geppi, M., et al. (2012). New LDPE based anion-exchange membranes for alkaline solid polymer electrolyte water electrolysis. *Int. J. Hydrogen Energy* 37 (20), 14992–15002. doi:10.1016/j.ijhydene.2012.08.012
- Galizia, M., Benedetti, F. M., Paul, D. R., and Freeman, B. D. (2017). Monovalent and divalent ion sorption in a cation exchange membrane based on cross-linked poly(p-styrene sulfonate-co-divinylbenzene). *J. Membr. Sci.* 535, 132–142. doi:10.1016/j.memsci.2017.04.007
- Gao, H., Li, J., Fu, R., Wang, L., Wang, H., Pan, T., et al. (2023). The effect of flow modes on the capture of the energy between concentrated brine and seawater by reverse electro dialysis. *Energy Convers. Manag.* 292, 117357. doi:10.1016/j.enconman.2023.117357
- Gao, H., Zhang, B., Tong, X., and Chen, Y. (2018). Monovalent-anion selective and antifouling polyelectrolytes multilayer anion exchange membrane for reverse electro dialysis. *J. Membr. Sci.* 567, 68–75. doi:10.1016/j.memsci.2018.09.035
- Geise, G. M., Hickner, M. A., and Logan, B. E. (2013). Ionic resistance and permselectivity tradeoffs in anion exchange membranes. *ACS Appl. Mater. Interfaces* 5 (20), 10294–10301. doi:10.1021/am403207w
- Golubenkov, D. V., Van der Bruggen, B., and Yaroslavtsev, A. B. (2019). Novel anion exchange membrane with low ionic resistance based on chloromethylated/quaternized-grafted polystyrene for energy efficient electromembrane processes. *J. Appl. Polym. Sci.* 137 (19), 48656. doi:10.1002/app.48656
- Golubenkov, D. V., Van der Bruggen, B., and Yaroslavtsev, A. B. (2021). Ion exchange membranes based on radiation-induced grafted functionalized polystyrene for high-performance reverse electro dialysis. *J. Power Sources* 511, 230460. doi:10.1016/j.jpowsour.2021.230460
- Guler, E., van Baak, W., Saakes, M., and Nijmeijer, K. (2014). Monovalent-ion-selective membranes for reverse electro dialysis. *J. Membr. Sci.* 455, 254–270. doi:10.1016/j.memsci.2013.12.054
- Guler, E., Zhang, Y., Saakes, M., and Nijmeijer, K. (2012). Tailor-made anion-exchange membranes for salinity gradient power generation using reverse electro dialysis. *ChemSusChem* 5 (11), 2262–2270. doi:10.1002/cssc.201200298
- Hagesteyn, K. F. L., Jiang, S., and Ladewig, B. P. (2018). A review of the synthesis and characterization of anion exchange membranes. *J. Mater. Sci.* 53 (16), 11131–11150. doi:10.1007/s10853-018-2409-y
- Han, J.-H., Jeong, H., Hwang, K. S., Kim, C.-S., Jeong, N., and Yang, S. (2020). Asymmetrical electrode system for stable operation of a large-scale reverse electro dialysis (RED) system. *Environ. Sci. Water Res. Technol.* 6, 1597–1605. doi:10.1039/D0EW00001A
- Han, J. H., Jeong, N., Kim, C. S., Hwang, K. S., Kim, H., Nam, J. Y., et al. (2019). Reverse electro dialysis (RED) using a bipolar membrane to suppress inorganic fouling around the cathode. *Water Res.* 166, 115078. doi:10.1016/j.watres.2019.115078
- Han, S. J., and Park, J. S. (2021). Understanding membrane fouling in electrically driven energy conversion devices. *Energies* 14 (1), 212. doi:10.3390/en14010212
- Hong, J. G., Zhang, B., Glabman, S., Uzal, N., Dou, X., Zhang, H., et al. (2015). Potential ion exchange membranes and system performance in reverse electro dialysis for power generation: a review. *J. Membr. Sci.* 486, 71–88. doi:10.1016/j.memsci.2015.02.039
- Hosseini, S., Jashni, E., Jafari, M., Bruggen, B., and Shahedi, Z. (2018). Nanocomposite polyvinyl chloride-based heterogeneous cation exchange membrane prepared by synthesized ZnQ2 nanoparticles: ionic behavior and morphological characterization. *J. Membr. Sci.* 560, 1–10. doi:10.1016/j.memsci.2018.05.007
- Jang, J., Kang, Y., Han, J.-H., Jang, K., Kim, C.-M., and Kim, I. S. (2020). Developments and future prospects of reverse electro dialysis for salinity gradient power generation: influence of ion exchange membranes and electrodes. *Desalination* 491, 114540. doi:10.1016/j.desal.2020.114540
- Jeong, J., Song, H., and Choi, I. (2021). Electrochemical analysis on how structural and compositional modification of electrode affects power generation in reverse electro dialysis. *Korean J. Chem. Eng.* 38, 170–178. doi:10.1007/s11814-020-0690-3
- Jwa, E., Kim, H., Nam, J. Y., Han, J. I., and Jeong, N. (2023). Design strategy of cathodic electrocatalysts to effectively suppress inorganic fouling for long-term stability of reverse electro dialysis. *Chem. Eng. J.* 476, 146521. doi:10.1016/j.cej.2023.146521
- Kang, M. S. (2013). Development of pore-filled ion-exchange membranes for efficient all vanadium redox flow batteries. *J. Korean Electrochem. Soc.* 16 (4), 204–210. doi:10.5229/jkes.2013.16.4.204
- Khoiruddin, A. D., Subagio, and Wenten, I. G. (2017). Surface modification of ion-exchange membranes: methods, characteristics, and performance. *J. Appl. Polym. Sci.* 134 (48), 45540. doi:10.1002/app.45540
- Kickelbick, G. (2003). Concepts for the incorporation of inorganic building blocks into organic polymers on a nanoscale. *Prog. Polym. Sci.* 28 (1), 83–114. doi:10.1016/s0079-6700(02)00019-9
- Kim, D. H., Park, J. S., Choun, M., Lee, J., and Kang, M. S. (2016). Pore-filled anion-exchange membranes for electrochemical energy conversion applications. *Electrochim. Acta* 222, 212–220. doi:10.1016/j.electacta.2016.10.041

Publisher's note

All claims expressed in this article are solely those of the authors and do not necessarily represent those of their affiliated organizations, or those of the publisher, the editors and the reviewers. Any product that may be evaluated in this article, or claim that may be made by its manufacturer, is not guaranteed or endorsed by the publisher.

- Kim, H. K., Lee, M. S., Lee, S. Y., Choi, Y. W., Jeong, N. J., and Kim, C. S. (2015). High power density of reverse electro dialysis with pore-filling ion exchange membranes and a high-open-area spacer. *J. Mater. Chem. A* 3, 16302–16306. doi:10.1039/C5TA03571F
- Kotoka, F., Merino-Garcia, I., and Velizarov, S. (2020). Surface modifications of anion exchange membranes for an improved reverse electro dialysis process performance: a review. *Membranes* 10 (8), 160. doi:10.3390/membranes10080160
- Lee, Y. J., Cha, M. S., Oh, S. G., So, S., Kim, T. H., Ryoo, W. S., et al. (2019). Reinforced anion exchange membrane based on thermal cross-linking method with outstanding cell performance for reverse electro dialysis. *RSC Adv.* 9 (47), 27500–27509. doi:10.1039/C9RA04984C
- Li, M., Zhang, N., Zheng, H., Guo, J., Xiang, Z., Lu, X., et al. (2024). Improved power production in reverse electro dialysis stacks with ion-permselective woven net spacers. *Energy Technol.* 2301215. doi:10.1002/ente.202301215
- Luo, T., Abdu, S., and Wessling, M. (2018). Selectivity of ion exchange membranes: a review. *J. Membr. Sci.* 555, 429–454. doi:10.1016/j.memsci.2018.03.051
- Mehdizadeh, S., Yasukawa, M., Abo, T., Kakihana, Y., and Higa, M. (2019). Effect of spacer geometry on membrane and solution compartment resistances in reverse electro dialysis. *J. Membr. Sci.* 572, 271–280. doi:10.1016/j.memsci.2018.09.051
- Mikhaylin, S., and Bazinet, L. (2016). Fouling on ion-exchange membranes: classification, characterization and strategies of prevention and control. *Adv. Colloid Interface Sci.* 229, 34–56. doi:10.1016/j.cis.2015.12.006
- Moya, A. A. (2020). Uphill transport in improved reverse electro dialysis by removal of divalent cations in the dilute solution: a Nernst-Planck based study. *J. Membr. Sci.* 598, 117784. doi:10.1016/j.memsci.2019.117784
- Moya, D., Aldas, C., and Kaparaju, P. (2018). Geothermal energy: power plant technology and direct heat applications. *Renew. Sust. Energ. Rev.* 94, 889–901. doi:10.1016/j.rser.2018.06.047
- Nazif, A., Saljoughi, E., Mousa, S., and Karkhanechi, H. (2023a). Embedding MXene nanosheets into cation exchange membranes to enhance power generation by reverse electro dialysis. *Desalination* 566, 116926. doi:10.1016/j.desal.2023.116926
- Nazif, A., Saljoughi, E., Mousa, S. M., and Karkhanechi, H. (2023b). Improved permselectivity and mechanical properties of sulfonated poly dimethyl phenylene oxide cation exchange membrane using MXene nanosheets. *Desalination* 549, 116329. doi:10.1016/j.desal.2022.116329
- Nemati, M., Hosseini, S. M., Bagheripour, E., and Madaeni, S. S. (2015). Electro dialysis heterogeneous anion exchange membranes filled with TiO₂ nanoparticles: membranes, fabrication and characterization. *J. Membr. Sci. Res.* 1 (3), 135–140. doi:10.22079/JMSR.2015.14485
- Othman, N. H., Alias, N. H., Fuzil, N. S., Marpani, F., Shahrudin, M. Z., Chew, C. M., et al. (2022a). A review on the use of membrane technology systems in developing countries. *Membranes* 12 (1), 30. doi:10.3390/membranes12010030
- Othman, N. H., Kabay, N., and Guler, E. (2022b). Principles of reverse electro dialysis and development of integrated-based system for power generation and water treatment: a review. *Rev. Chem. Eng.* 38 (8), 921–958. doi:10.1515/revce-2020-0070
- Park, J. S., Lee, H. J., Choi, S. J., Geckeler, K. E., Cho, J., and Moon, S. H. (2003). Fouling mitigation of anion exchange membrane by zeta potential control. *J. Colloid Interface Sci.* 259 (2), 293–300. doi:10.1016/S0021-9797(02)00095-4
- Pawlowski, S., Crespo, J. G., and Velizarov, S. (2019). Profiled ion exchange membranes: a comprehensive review. *Int. J. Mol. Sci.* 20 (1), 165. doi:10.3390/ijms20010165
- Pintossi, D., Saakes, M., Borneman, Z., and Nijmeijer, K. (2021). Tailoring the surface chemistry of anion exchange membranes with zwitterions: toward antifouling red membranes. *ACS Appl. Mater. Interfaces* 13 (15), 18348–18357. doi:10.1021/acsami.1c02789
- Post, J. W., Hamelers, H. V., and Buisman, C. J. (2009). Influence of multivalent ions on power production from mixing salt and fresh water with a reverse electro dialysis system. *J. Membr. Sci.* 330, 65–72. doi:10.1016/j.memsci.2008.12.042
- Post, J. W., Hamelers, H. V. M., and Buisman, C. J. N. (2008). Energy recovery from controlled mixing salt and fresh water with a reverse electro dialysis system. *Environ. Sci. Technol.* 42, 5785–5790. doi:10.1021/es8004317
- Post, J. W., Veerman, J., Hamelers, H. V. M., Euverink, G. J. W., Metz, S. J., Nijmeijer, K., et al. (2007). Salinity gradient power: evaluation of pressure-retarded osmosis and reverse electro dialysis. *J. Membr. Sci.* 288, 218–230. doi:10.1016/j.memsci.2006.11.018
- Qaisrani, N. A., Ma, Y., Ma, L., Liu, J., Gao, L., Li, L., et al. (2018). Facile and green fabrication of polybenzoxazine-based composite anion-exchange membranes with a self-cross-linked structure. *Ionics* 24 (10), 3053–3063. doi:10.1007/s11581-017-2433-y
- Sankar, S., Roby, S., Kuroki, H., Miyaniishi, S., Tamaki, T., Anilkumar, G. M., et al. (2022). High-performing anion exchange membrane water electrolysis using self-supported metal phosphide anode catalysts and an ether-free aromatic polyelectrolyte. *ACS Sustain. Chem. Eng.* 11 (3), 854–865. doi:10.1021/acsschemeng.2c03663
- Santoro, S., Tufa, R. A., Avci, A. H., Fontananova, E., Di Profio, G., and Curcio, E. (2021). Fouling propensity in reverse electro dialysis operated with hypersaline brine. *Energy* 228, 120563. doi:10.1016/j.energy.2021.120563
- Siekierka, A., and Yalcinkaya, F. (2022). Selective cobalt-exchange membranes for electro dialysis dedicated for cobalt recovery from lithium, cobalt and nickel solutions. *Sep. Purif. Technol.* 299, 121695. doi:10.1016/j.seppur.2022.121695
- Siekierka, A., Yalcinkaya, F., and Bryjak, M. (2023). Recovery of transition metal ions with simultaneous power generation by reverse electro dialysis. *J. Environ. Chem. Eng.* 11 (3), 110145. doi:10.1016/j.jece.2023.110145
- Simões, C., Pintossi, D., Saakes, M., and Brillman, W. (2021). Optimizing multistage reverse electro dialysis for enhanced energy recovery from river water and seawater: experimental and modeling investigation. *Adv. Appl. Energy* 2, 100023. doi:10.1016/j.adapen.2021.100023
- Simões, C., Saakes, M., and Brillman, D. (2023). Toward redox-free reverse electro dialysis with carbon-based slurry electrodes. *Ind. Eng. Chem. Res.* 62 (3), 1665–1675. doi:10.1021/acs.iecr.2c03567
- Simões, C., Vital, B., Sleutels, T., Sleutels, T., Saakes, M., and Brillman, W. (2022). Scaled-up multistage reverse electro dialysis pilot study with natural waters. *Chem. Eng. J.* 450, 138412. doi:10.1016/j.cej.2022.138412
- Song, H. B., Kim, D. H., and Kang, M. S. (2022). Thin-reinforced anion-exchange membranes with high ionic contents for electrochemical energy conversion processes. *Membranes* 12 (2), 196. doi:10.3390/membranes12020196
- Tiago, G., Cristóvão, M. B., Marques, A. P., Huertas, R., Merino-García, I., Pereira, V. J., et al. (2022). A study on biofouling and cleaning of anion exchange membranes for reverse electro dialysis. *Membranes* 12 (7), 697. doi:10.3390/membranes12070697
- Tong, X., Zhang, B., and Chen, Y. (2016). Fouling resistant nanocomposite cation exchange membrane with enhanced power generation for reverse electro dialysis. *J. Membr. Sci.* 516, 162–171. doi:10.1016/j.memsci.2016.05.060
- Tufa, R., Piallat, T., Hnát, J., Fontananova, E., Paidar, M., Chanda, D., et al. (2020). Salinity gradient power reverse electro dialysis: cation exchange membrane design based on polypyrrole-chitosan composites for enhanced monovalent selectivity. *Chem. Eng. J.* 380, 122461. doi:10.1016/j.cej.2019.122461
- Tufa, R. A., Pawlowski, S., Veerman, J., Bouzek, K., Fontananova, E., di Profio, G., et al. (2018). Progress and prospects in reverse electro dialysis for salinity gradient energy conversion and storage. *Appl. Energy* 225, 290–331. doi:10.1016/j.apenergy.2018.04.111
- Varcoe, J. R., Atanassov, P., Dekel, D. R., Herring, A. M., Hickner, M. A., Kohl, P. A., et al. (2014). Anion-exchange membranes in electrochemical energy systems. *Energy Environ. Sci.* 7 (10), 3135–3191. doi:10.1039/c4ee01303d
- Vermaas, D., Kunteng, D., Saakes, M., and Nijmeijer, K. (2013). Fouling in reverse electro dialysis under natural conditions. *Water Res.* 47 (3), 1289–1298. doi:10.1016/j.watres.2012.11.053
- Vermaas, D. A., Saakes, M., and Nijmeijer, K. (2011a). Doubled power density from salinity gradients at reduced intermembrane distance. *Environ. Sci. Technol.* 45, 7089–7095. doi:10.1021/es2012758
- Vermaas, D. A., Saakes, M., and Nijmeijer, K. (2011b). Power generation using profiled membranes in reverse electro dialysis. *J. Membr. Sci.* 385–386, 234–242. doi:10.1016/j.memsci.2011.09.043
- Vermaas, D. A., Saakes, M., and Nijmeijer, K. (2014). Enhanced mixing in the diffusive boundary layer for energy generation in reverse electro dialysis. *J. Membr. Sci.* 453, 312–319. doi:10.1016/j.memsci.2013.11.005
- Vital, B., Sleutels, T., Gagliano, M. C., and Hamelers, H. V. M. (2023). Reversible fouling by particulate matter from natural seawater reduces RED performance while limiting biofouling. *Desalination* 548, 116262. doi:10.1016/j.desal.2022.116262
- Wang, L., Zhao, Y., Long, R., Liu, Z., and Liu, W. (2024). Techno-economics of multi-stage reverse electro dialysis for blue energy harvesting. *Carb. Neutrality* 3, 12. doi:10.1007/s43979-024-00087-7
- Xu, T. (2005). Ion exchange membranes: state of their development and perspective. *J. Membr. Sci.* 263 (1–2), 1–29. doi:10.1016/j.memsci.2005.05.002
- Yang, K., Xu, J., Shui, T., Zhang, Z., Wang, H., Liu, Q., et al. (2020). Cross-linked poly (aryl ether ketone) anion exchange membrane with high ion conductivity by two different functional imidazole side chain. *React. Funct. Polym.* 151, 104551. doi:10.1016/j.reactfunctpolym.2020.104551
- Zarfl, C., Lumsdon, A. E., Berlekamp, J., Tydecks, L., and Tockner, K. (2015). A global boom in hydropower dam construction. *Aquat. Sci.* 77, 161–170. doi:10.1007/s00027-014-0377-0
- Zhang, H., Jiang, D., Zhang, B., Hong, J., and Chen, Y. (2017). A novel hybrid poly (vinyl alcohol) (PVA)/Poly (2,6-dimethyl-1,4-phenylene oxide) (PPO) membranes for reverse electro dialysis power system. *Electrochim. Acta* 239, 65–73. doi:10.1016/j.electacta.2017.04.008
- Zhao, Y., Li, Y., Yuan, S., Zhu, J., Houtmeyers, S., Li, J., et al. (2019). A chemically assembled anion exchange membrane surface for monovalent anion selectivity and fouling reduction. *J. Mater. Chem. A* 7 (11), 6348–6356. doi:10.1039/c8ta11868j
- Zhao, Z., Shi, S., Cao, H., Li, Y., and Van der Bruggen, B. (2018). Layer-by-layer assembly of anion exchange membrane by electrodeposition of polyelectrolytes for improved antifouling performance. *J. Membr. Sci.* 558, 1–8. doi:10.1016/j.memsci.2018.04.035
- Zhu, J., Liao, J., Jin, W., Luo, B., Shen, P., Sotto, A., et al. (2019). Effect of functionality of cross-linker on sulfonated polysulfone cation exchange membrane for electro dialysis. *React. Funct. Polym.* 138, 104–113. doi:10.1016/j.reactfunctpolym.2019.02.006
- Zuo, P., Xu, Z., Zhu, Q., Ran, J., Ge, L., Ge, X., et al. (2022). Ion exchange membranes: constructing and tuning ion transport channels. *Adv. Funct. Mater.* 32 (52), 2207366. doi:10.1002/adfm.202207366